

---

# AIS/VDES R-mode Development

## Technical Report

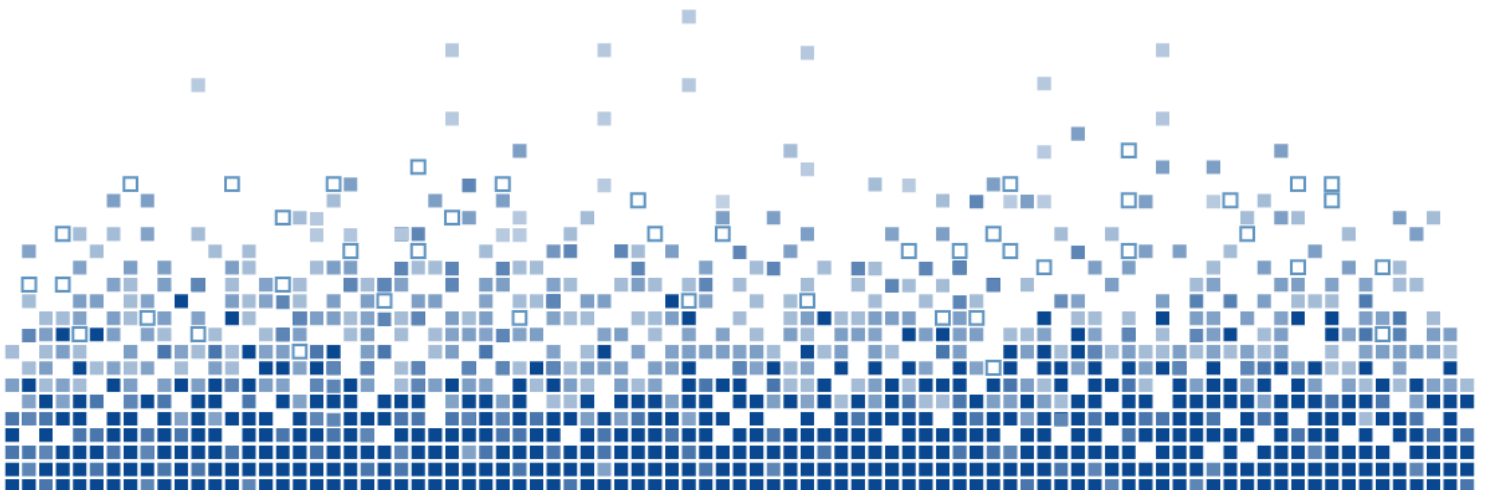
Report No: RPT-29-JSa-18

Report Version: 1.1

Report Version Date: 29/08/2018

GLA/DfT Confidential

© Research & Radionavigation Directorate, The Quay, Harwich, CO12 3JW - 29/08/2018



Lead Author	Reviewer	Approved for Release
Jan Safar	NW, AG, PW	Name
R&D Engineer	Job Title	Job Title
JS	Signature	Signature

Please make comments in this box:

**Report for website:**

*This report presents a detailed literature review on AIS/VDES R-mode, followed by an overview of the key areas that remain to be addressed, including the user requirements, system architecture, base station and user equipment considerations and the need for modification of equipment standards and regulations. A preliminary theoretical analysis of VDES ranging performance is carried out and recommendations for future work are given.*

*Theoretical bounds on the ranging performance are derived for both the AIS and new VDES waveforms and plots of estimated ranging error vs. distance are provided for two representative antenna heights. Maximum usable base station ranges are estimated for the different AIS/VDES waveforms, assuming a positioning accuracy requirement in the low tens of meters. The estimated maximum station range figures, along with the known distribution of existing AIS base stations in the UK and Ireland, are used to provide an initial estimate of the achievable AIS and VDES R-mode coverage in the waters around the British Isles.*

*Results of this analysis suggest that there is an insufficient number of base stations to provide a 10 m-level AIS R-mode service coverage along the UK and Irish coasts. The analysis further suggests that if all existing AIS base stations are converted to VDES, then there may be sufficient station availability to enable 10 m-level positioning along the north and west coast of Scotland, south-east of England and along a significant portion of the Irish coastline. However, even with the new VDES waveforms, additional base stations would need to be deployed in certain parts of the GLA service area in order to achieve contiguous coverage.*

*The need for new base stations could be minimised by implementing active (two-way) ranging and/or including a high-stability clock in the R-mode user equipment. Plots are provided in the report illustrating the difference in achievable coverage when passive vs. active ranging is used.*

## Executive Summary

In the context of maritime navigation, R-mode refers to the use of existing or new maritime radio communications infrastructure for ranging. The aim is to mitigate the impact of disruptions to Global Navigation Satellite System (GNSS) services on maritime navigation, while minimising the deployment costs.

Ranging systems work by measuring the time of arrival of signals from fixed radio transmitters and using this information to estimate the distance between the user and the transmitter(s). If sufficient transmitters are available, the user's position can be calculated by multilateration. Measurements from multiple ranging systems, including GNSS and terrestrial systems such as eLoran, can be combined to form a single resilient position, velocity and time solution, as envisaged in IMO Resolution MSC.401(95).

Two concepts for R-mode are currently being studied by the international maritime community; one using the medium-frequency signals of the IALA Marine Beacon DGPS system, the other one making use of base station networks of the Automatic Identification System (AIS) and its planned successor, the VHF Data Exchange System (VDES). The focus of this study is on the AIS/VDES R-mode.

This report presents a detailed literature review on AIS/VDES R-mode, followed by an overview of the key areas that remain to be addressed, including the user requirements, system architecture, base station and user equipment considerations and the need for modification of equipment standards and regulations. A preliminary theoretical analysis of VDES ranging performance is carried out and recommendations for future work are given.

Theoretical bounds on the ranging performance are derived in the report for both the AIS and new VDES waveforms and plots of estimated ranging error vs. distance are provided for two representative antenna heights. The theoretical analysis shows that all of the new VDES waveforms can be expected to provide better ranging performance than the AIS waveform. The best performance is achieved using the 100 kHz bandwidth VDES waveforms which provide approximately five to twelve-times lower one-sigma ranging error than the AIS (depending on the transmission configuration).

Maximum usable base station ranges are estimated for the different AIS/VDES waveforms, assuming a positioning accuracy requirement in the low tens of meters. Under this assumption, the maximum range for an AIS-based R-mode station is expected to be between 10 NM and 15 NM (depending on the antenna heights). If one of the new 100 kHz bandwidth VDES waveforms is used instead of AIS, the maximum range is expected to increase to about 25 NM to 34 NM.

The estimated maximum station range figures, along with the known distribution of existing AIS base stations in the UK and Ireland, are used to provide an initial estimate of the achievable AIS and VDES R-mode coverage in the waters around the British Isles. Results of this analysis suggest that there is an insufficient number of base stations to provide a 10 m-level AIS R-mode service coverage along the UK and Irish coasts. The analysis further suggests that if all existing AIS base stations are converted to VDES, then there may be sufficient station availability to enable 10 m-level positioning along the north and west coast of Scotland, south-east of England and along a significant portion of the Irish coastline. However, even with the new VDES waveforms, additional base stations would need to be deployed in certain parts of the GLA service area in order to achieve contiguous coverage.

The need for new base stations could be minimised by implementing active (two-way) ranging and/or including a high-stability clock in the R-mode user equipment. Plots are provided in the report illustrating the difference in achievable coverage when passive vs. active ranging is used.

Caveat: the theoretical predictions in this report do not include the effects of multipath propagation, base station synchronisation error and transmission jitter, changing environmental conditions and terrain topography. These factors will be addressed in a future report. A comparison with experimental results for AIS R-mode published by the Dalian Maritime University confirms that the theoretical model generally underestimates the measurement error obtained in a real-world setting. It should also be noted that the preliminary coverage plots are based purely on signal availability and do not take transmitter-receiver geometry into account.

Given the results of this study, it is recommended that future work should:

1. Focus on VDES R-mode rather than AIS R-mode (noting that VDES includes AIS).
2. Determine the achievable ranging performance under realistic propagation conditions and transmitter-receiver separations through further theoretical analysis and measurement.
3. Review the user requirements for VDES R-mode and consolidate system requirements.
4. Propose a system architecture for VDES R-mode.
5. Model the coverage and performance for the proposed system architecture(s) and estimate the cost of the necessary infrastructure, user equipment and operation.
6. Repeat steps 3. to 5. to determine the optimal system architecture.

Further detailed recommendations are provided in the report.

## Document Disclaimer

This document is uncontrolled when removed from iManage (either electronic or printed)

## Document Information

Client	GLA
Project Title	AIS/VDES R-mode Development
Deliverable Number	M062/2016
Report Title	AIS/VDES R-mode Development – Technical Report
Report Identifier	RPT-29-JSa-18
Report Version	1.1
Report Version Date	29/08/2018
Lead Author	Dr Jan Šafář
Lead Author's Contact Information	GLA Research and Radionavigation The Quay, Harwich, Essex, CO12 3JW, UK T: +44-1255-24EXT E: @gla-rnav.org W: www.gla-rnav.org
Contributing Author(s)	
iManage Location	
Circulation	<ol style="list-style-type: none"> <li>1. Client</li> <li>2. Project Files (hard copy)</li> <li>3. R&amp;RNAV Distribution List</li> <li>4. R&amp;RNAV Team</li> </ol>

## Contents

1	Introduction .....	10
2	Literature Review .....	10
2.1	System Architecture .....	10
2.2	Base Station Considerations .....	12
2.2.1	Signal Structure .....	12
2.2.2	Synchronisation .....	12
2.2.3	Availability of Base Stations and Station Geometry .....	13
2.2.4	Standards Modification and Limitations of Existing Equipment .....	13
2.3	Propagation Channel .....	14
2.3.1	Received Signal Strength .....	14
2.3.2	Radio Noise .....	14
2.3.3	Multipath Propagation .....	14
2.3.4	'Additional Secondary Factors' .....	15
2.3.4.1	Preliminary Analysis of the Effect of Environmental Factors on Propagation Delay .....	15
2.4	User Equipment Considerations .....	17
2.4.1	Ranging Algorithms and Theoretical Bounds on Ranging Performance .....	17
2.4.2	Position Calculation and Theoretical Bounds on Positioning Performance .....	18
2.4.3	Standards Modifications and Limitations of Existing Equipment .....	18
2.5	Experimental Verification .....	18
3	Identification of Gaps and Next Steps .....	20
3.1	Requirements Capture .....	20
3.2	System Architecture .....	20
3.3	Base Station Considerations .....	23
3.3.1	Signal Structure .....	23
3.3.2	Synchronisation .....	23
3.3.3	Availability of Base Stations and Station Geometry .....	23
3.3.4	Standards Modifications and Limitations of Existing Equipment .....	23
3.4	Propagation Channel .....	23
3.4.1	Multipath Propagation .....	23
3.4.2	Radio Noise / Interference .....	23
3.4.3	'ASFs' .....	23
3.5	User Equipment Considerations .....	24
3.5.1	Ranging Algorithms and Theoretical Bounds on Ranging Performance .....	24
3.5.2	Position Calculation and Theoretical Bounds on Positioning Performance .....	24

3.5.3	Standards Modifications and Limitation of Existing Equipment.....	24
3.6	Experimental Verification .....	24
3.7	Recommended Next Steps – A Development Roadmap .....	25
4	Preliminary Theoretical Analysis of VDES Ranging Performance.....	28
4.1	VDES R-mode Signal Specification .....	28
4.1.1	VDES Subsystems and their Suitability for R-mode .....	28
4.1.2	VDES Modulations.....	28
4.1.2.1	GMSK .....	29
4.1.2.2	PSK/QAM.....	30
4.1.3	Symbol Rate .....	31
4.1.4	Transmission Duration and Number of Symbols used for Range Estimation..	31
4.1.5	Data Sequence .....	32
4.2	VDES Propagation Channel Model .....	33
4.3	Bounds on Ranging Performance .....	33
4.3.1	Modified Cramér-Rao Bound for AIS/VDES R-mode.....	34
4.3.1.1	GMSK (AIS) .....	34
4.3.1.2	PSK/QAM (VDES).....	35
4.3.1.3	GMSK (AIS) vs. PSK/QAM (VDES) Comparison .....	37
4.3.1.4	Receiver Integration .....	38
4.3.2	Ranging Performance vs. Distance.....	40
4.3.2.1	Received Power vs. Distance .....	40
4.3.2.2	Radio Noise.....	42
4.3.2.3	Ranging Error vs. Distance.....	46
4.4	Discussion .....	50
4.4.1	Comparison with the ACCSEAS AIS R-mode Model.....	50
4.4.2	Comparison with Measurement Results.....	51
4.4.3	Maximum Usable Range and Achievable Coverage .....	51
5	Recommendations for Future Work.....	54
	References .....	55

## List of Figures

Figure 1: AIS Autonomous Positioning System (AAPS) architecture, including the 'Additional Secondary Factor Correction' subsystem [3].	11
Figure 2: AIS/VDES ranging error vs. carrier-power-to-noise-density ratio assuming one-slot transmissions.	38
Figure 3: AIS/VDES ranging error vs. carrier-power-to-noise-density ratio assuming maximum-length transmissions.	39
Figure 4: AIS / VDES ranging error vs. carrier-power-to-noise-density ratio assuming one-slot transmissions and receiver integration over five slots.	40
Figure 5: Received power vs. distance for a 12.5 W ERP VHF transmission, using a receiving antenna with a gain of 0 dBd (2.15 dBi).	42
Figure 6: Noise-equivalent model of the system.	45
Figure 7: Ranging error vs. distance; one-slot bursts; base station ant. height: 18 m.	47
Figure 8: Ranging error vs. distance; one-slot bursts; base station ant. height: 57 m.	47
Figure 9: Ranging error vs. distance; maximum-length bursts; base station antenna height: 18 m.	48
Figure 10: Ranging error vs. distance; maximum-length bursts; base station antenna height: 57 m.	48
Figure 11: Ranging error vs. distance; one-slot bursts; receiver integration over 5 slots; base station ant. height: 18 m.	49
Figure 12: Ranging error vs. distance; one-slot bursts; receiver integration over 5 slots; base station ant. height: 57 m.	49
Figure 13: Simultaneous availability of 3 (left) and 2 (right) R-mode base stations (supporting positioning by passive and active ranging, resp.), assuming maximum usable station range of 15 NM (AIS waveform).	53
Figure 14: Simultaneous availability of 3 (left) and 2 (right) R-mode base stations (supporting positioning by passive and active ranging, resp.), assuming maximum usable station range of 34 NM (VDE-TER 100K waveforms).	53

## List of Tables

Table 1: Environmental data from the Liaoning weather monitoring station, Dalian, China; min/max values over the period of January 2009 to February 2018 are shown. ....	16
Table 2: Partial pressure of water vapour estimated based on environmental data from the Liaoning weather monitoring station, Dalian, China; min/max values over the period of January 2009 to February 2018 are shown.....	16
Table 3: Example VDES R-mode system architectures.....	21
Table 4: Some pros and cons of the example VDES R-mode system architectures.....	22
Table 5: VDES modulations. ....	29
Table 6: RRC roll-off factor values used in VDES. ....	31
Table 7: Symbol rates for different VDES subsystem configurations. ....	31
Table 8: Potential VDES R-mode transmission configurations. ....	32
Table 9: Ranging error coefficients for different VDES transmission formats.....	37
Table 10: Number of symbols per observation for the one-slot burst transmission configuration with receiver integration. ....	39
Table 11: Assumptions related to received power modelling. ....	41
Table 12: Parameters of the linear model of the median man-made noise [31]. ....	43
Table 13: Parameters of the linear model of the vessel's topside noise.....	44
Table 14: Comparison of the proposed model for AIS ranging error with the ACCSEAS model. ....	50
Table 15: Comparison of the proposed AIS ranging error model with experimental results published by the DMU.....	51
Table 16: Estimated maximum transmitter-receiver separation for 10 m ranging error.....	52

## 1 Introduction

In the context of maritime navigation, R-mode refers to the use of existing or new maritime radio communications infrastructure for ranging. The aim is to mitigate the impact of disruptions to Global Navigation Satellite System (GNSS) services on maritime navigation, while minimising the deployment costs.

Ranging systems work by measuring the time of arrival of signals from fixed radio transmitters and using this information to estimate the distance between the user and the transmitter(s). If sufficient transmitters are available, the user's position can be calculated by multilateration. Measurements from multiple ranging systems, including GNSS and terrestrial systems such as eLoran, can be combined to form a single resilient position, velocity and time solution, as envisaged in IMO Resolution MSC.401(95).

Two concepts for R-mode are currently being studied by the international maritime community; one using the medium-frequency signals of the IALA Marine Beacon DGPS system, the other one making use of base station networks of the Automatic Identification System (AIS) and its potential successor, the VHF Data Exchange System (VDES). The focus of this study is on the AIS/VDES R-mode.

This report presents a detailed literature review on AIS/VDES R-mode, followed by an overview of the key areas that remain to be addressed. A preliminary theoretical analysis of VDES ranging performance is carried out and recommendations for future work are given.

## 2 Literature Review

The literature on AIS R-mode is relatively sparse. The technique was first studied by the ACCSEAS project [1], [2] and more recently by a group of researchers at the Dalian Maritime University (DMU), China [3]–[6]. It is also known that at least one AIS equipment manufacturer previously investigated the feasibility of AIS R-mode and a similar technology, enabling the localisation of a vessel using a network of shore-based AIS receivers, was patented by another manufacturer [7].

This section provides an overview of the key findings of the previous R-mode studies, organised under the following headings: system architecture, base station considerations, propagation channel characteristics, receiver considerations and experimental verification.

### 2.1 System Architecture

**The ACCSEAS R-mode study [1] proposed four candidate R-mode architectures:**

- A. 'Status Quo' – ranging off existing AIS messages (Message 4 – base station message) or additional AIS messages (Message 8);
- B. Use of additional VHF maritime channel(s) in conjunction with pulsed, Continuous Wave (CW) or 'two-tone modulation' ranging signals;
- C. Adding ranging signals (same as above) on the AIS channels; and
- D. Use of a wideband modulation, e.g. a very low-level spread-spectrum signal transmitted across the entire or most of the maritime VHF band.

An assumption common to all of the candidate architectures was that the transmitters are provided with a high-quality clock and are all synchronized to a common timing source (synchronizing both times of symbol transitions and carrier frequency and phase as well as appropriate parameters of any other signals being transmitted).

A preliminary evaluation recommended the following three architectural options for further investigation [1]:

- A2. AIS Message 8 transmissions, noting that high precision will probably not be possible due to the inability to resolve carrier phase ambiguities;
- B2. CW signals on one or more distinct VHF channels; and
- D1. Spread spectrum signal across the available portions of the maritime VHF band.

A follow-on report [2] presented a theoretical analysis of the achievable ranging and positioning accuracy performance for the three short-listed options and **recommended that the 'AIS Message 8' architecture (option A2 above) be taken forward** for further analysis. The evaluation was based on using 60 AIS slots per minute, increasing the AIS VHF Data Link (VDL) loading by 1.3% (per R-mode base station). The report also noted that improved performance could be achieved using higher bandwidth transmissions on the *VHF Data Exchange System* (VDES) channels.

Building on the findings of the ACCSEAS study, researchers at the **DMU augmented the preferred ACCSEAS architecture with an 'ASF Correction' subsystem**, as illustrated in Figure 1 and described in detail in references [3], [6]. The goal of this subsystem was to measure the variations in the propagation delay of the VHF signal across a fixed baseline and generate real-time propagation corrections (these are, incorrectly, termed 'Additional Secondary Factors' in the literature, by analogy to eLoran ASFs). The corrections would be broadcast to users via AIS and would help eliminate measurement errors due to changing environmental factors affecting the signal propagation speed. For a further discussion of the AIS 'ASFs' see Section 2.3.4 of this document.

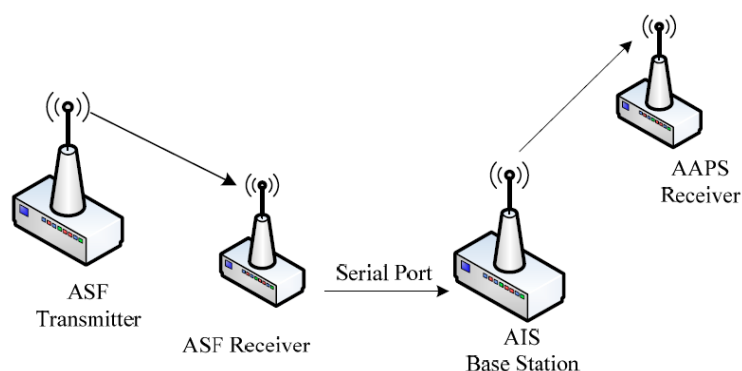


**Figure 1: AIS Autonomous Positioning System (AAPS) architecture, including the 'Additional Secondary Factor Correction' subsystem [3].**

The DMU paper [4] also mentions the possibility of using VDES for ranging.

Report [8] prepared for the GLA by University College London made the following key observations with respect to AIS R-mode architecture:

- **Without offshore beacons, positioning accuracy using passive AIS ranging will be significantly degraded due to poor solution geometry. The need for offshore beacons could be removed by implementing two-way (active) ranging.** In two-way ranging, the range is measured in both directions between a mobile user and a beacon at a known location. The two pseudo-ranges have equal and opposite timing biases, so the range may be obtained by taking their average. Consequently, no synchronization of the clocks is required, provided they are relatively stable. As a result, a position may be determined using one fewer beacon than required by passive ranging. For passive ranging, the beacons must surround the user to obtain good geometry, whereas for two-way ranging, they need only subtend 90°. However, this would require additions to the AIS transmission protocols, increase the system loading and limit the number of ships that can determine their position simultaneously. IMO

Resolution A.1046(27) states that 'systems should be capable of being used by an unlimited number of ships' and this may rule out two-way ranging.

- **Additionally, if ships were equipped with high quality clocks** using an Oven-Controlled Crystal Oscillator (OCXO) or Chip-Scale Atomic Clock (CSAC), **passive ranging could be used most of the time with relatively infrequent two-way ranging measurements to maintain clock calibration**; this would reduce the AIS loading considerably. Note that all AIS beacons would have to support two-way ranging to enable the clock to be calibrated.
- Further, the need for significant beacon densification could be reduced by augmenting AIS R-mode positioning with VHF and UHF signals of opportunity.

## 2.2 Base Station Considerations

### 2.2.1 Signal Structure

The ACCSEAS report [1] provided an overview of the AIS signal structure and basic characteristics of the AIS GMSK (Gaussian Minimum Shift Keying) modulation. In particular it was noted that:

- The AIS 1 and 2 channels are shared using Time Division Multiple Access (TDMA); the system is organised into time slots (of which there are 2,250 per minute);
- AIS transmission bursts can occupy a maximum of five consecutive slots;
- The AIS transmissions are typically synchronised to UTC; for a base station, transmission timing error should be within  $\pm 52 \mu\text{s}$  of the synchronisation source (corresponding to a range uncertainty of  $\pm 15.6 \text{ km}$ ) [9];
- AIS messages start with a known 32-bit training sequence which could be used for signal time of arrival estimation;
- AIS base stations transmit Message 4 (Base Station Report) at an interval of 10 seconds, alternating channels; if operating in 'semaphore mode', the interval decreases to 3.33 seconds; Message 4 occupies one time slot.

The follow-on report [2] also considered using AIS Message 8 transmissions (Binary Broadcast), which can occupy up to five slots and allow for more frequent broadcasts with a known structure (improving the ranging performance and position update rate).

### 2.2.2 Synchronisation

In order to do positioning from multiple ranges, the times of transmission must be accurately synchronised. The ACCSEAS report [2] assessed the requirements for a synchronisation source for an R-mode station as follows:

- Short-term clock stability at the transmitter of  $1 \times 10^{-10}$  is sufficient; this would argue for a Rubidium clock rather than a Caesium clock;
- Transmitter synchronisation to within 50 ns – 100 ns of a common reference such as UTC is required; this could potentially be done using a network time synchronisation protocol, Two-Way Satellite Time Transfer, eLoran, or GPS backed up by a Caesium clock.

The report also notes that the alternative to synchronising each transmitter is to have one or more reference sites that can determine the relative time differences between the various transmitters. This data would then need to be broadcast to users, possibly via the same signal used for ranging.

The DMU paper [3] recommends using a GPS-disciplined Rubidium clock for transmitter synchronisation, stating that 300 ns deviation per 24 hours in holdover mode and 30 ns deviation when disciplined were achieved experimentally.

### 2.2.3 Availability of Base Stations and Station Geometry

The ACCSEAS report [2] investigated base station availability and geometry for passive ranging along the north coast of Germany and around Denmark, where a relatively dense network of AIS base stations is currently in operation. Additionally, the stations considered in the study are nearly uniformly distributed across the analysis area, providing good transmitter-receiver geometries. HDOP<sup>1</sup> (Horizontal Dilution of Precision) plots were generated under the assumption of a maximum station range of 75 km (41 NM), providing a signal strength at that distance of greater than -117 dBm (the assumed sensitivity of the R-mode receiver). Due to the relatively long assumed station range and near-uniform distribution of stations across the analysis area, most of the area was shown to have HDOP of less than 2.

Note: the predicted ranging precision at the power level of -117 dBm is around 700 m (one sigma) [2] (compared to the positioning accuracy target of ~10 m), therefore it is questionable whether such a long range should have been used in the HDOP calculations.

Note also that the availability of base stations and the resulting transmitter-receiver geometry in the waters around the UK and Ireland are likely to be considerably less favourable than in the ACCSEAS analysis area, as discussed further in Section 4.4.2 of the current report.

The availability of (potential) R-mode base stations along the coast of China was studied in paper [4] by the DMU. Here, a maximum station range of 90 km (49 NM) was assumed. Despite this optimistic assumption, a great number of areas with insufficient coverage were identified, and the following options for improving station availability were discussed:

- Deploy new AIS base stations;
- Make use of AIS AtoN stations;
- Use MF DGNSS and Changhe II<sup>2</sup> reference stations as new R-mode beacon sites.

### 2.2.4 Standards Modification and Limitations of Existing Equipment

The ACCSEAS report [2] identified some AIS system modifications (both transmitter and receiver) that would be required in order to support AIS R-mode. The report states that no base station hardware modifications are required to support the 'AIS Message 8' R-mode architecture and makes the assumption that the transmission timing jitter can be eliminated by providing an external timing source. However, this assumption has been challenged in the following statement provided to the author by one of the major AIS equipment manufacturers:

'The transmission jitter requirement for an AIS base station is 54 micro seconds. Actual performance may be somewhat better, but this is the requirement.

A GPS receiver is typically used as a timing source, and this can be expected to provide 1PPS timing in the accuracy range of 50-200ns. (50ns is common today)

**Some base stations may allow for external 1PPS timing input. But it is not likely that this will improve the transmission jitter even if the external 1PPS accuracy is better than the base station internal GPS 1PPS signal,** as the 1PPS accuracy is most likely not the limiting factor.

The purpose of external 1PPS input may be as a backup in case of GPS dropouts, or to share a common timing source with other equipment on the same site.

1PPS must always be aligned with UTC when used in AIS applications.'

---

<sup>1</sup> HDOP is a term used in radionavigation to specify the multiplicative effect of navigation beacon geometry on positional measurement precision. Multiplying the standard deviation of the range measurement error by HDOP gives an estimate of the position error.

<sup>2</sup> Changhe II is a terrestrial hyperbolic positioning system developed by China in the 1980s, which ensures the navigational positioning of maritime vessels within a range of 1,300 nautical miles [10].

It seems likely that the above statement is valid for other manufacturers' equipment too, although this remains to be verified.

The statement also seems to be consistent with Recommendation ITU-R M.1371 (the technical specification for AIS), which states:

'For a base station, transmission timing error should be within  $\pm 52 \mu\text{s}$  of the synchronization source';

in other words, no matter how accurate the external synchronisation source is, the time of transmission of the AIS bursts may still be in error by  $\pm 52 \mu\text{s}$  (corresponding to a ranging error of  $\pm 15.6 \text{ km}$ ).

Therefore, **changes to the AIS specification and existing base station designs would likely be required in order to enable transmission synchronisation down to the  $\sim 10 \text{ ns}$  level required for accurate R-mode positioning.** Further modifications would likely be required in order to support active (two-way) ranging.

The VDES technical specification [11] currently requires that:

'the [transmission] timing jitter should be better than 5% of the symbol interval (peak value)'.

This corresponds to a peak error of approximately  $0.65 \mu\text{s}$  (195 m) for the highest VDES symbol rate and  $5.2 \mu\text{s}$  (1563 km) for the lowest rate; therefore, **changes would also need to be made to the VDES specification.**

## 2.3 Propagation Channel

### 2.3.1 Received Signal Strength

The received signal strength, along with the radio noise at the receiver, are the two key factors determining the ranging performance and the maximum usable station range. Models for the median signal strength for the VHF band for both sea-water and land-based propagation paths are available from the ITU [12], [13] and were implemented by the author in previous projects.

The ACCSEAS R-mode study [2] used a terrain-specific propagation prediction model (namely the Terrain Integrated Rough Earth Model developed by Alion), also taking into account directional antenna characteristics.

### 2.3.2 Radio Noise

The ACCSEAS R-mode study [2] considered two sources of radio noise when modelling R-mode performance: (i) thermal noise generated in the receiver; and (ii) man-made noise emanating from sources external to the receiver.

The thermal noise was modelled as Additive White Gaussian Noise (AWGN) with a power spectral density of  $kT_0 = -174 \text{ dBm/Hz}$  ( $k$  is the Boltzmann's constant and  $T_0$  is the reference temperature in degrees Kelvin, usually assumed to be 290 K).

The median man-made noise was estimated to be 15.8 dB, 11.4 dB and 6.1 dB above the thermal noise floor for business, residential and rural environments, respectively, based on a model provided in Recommendation ITU-R P.372. However, the noise level actually used in the performance analysis was based on the required Packet Error Rate at the minimum signal strength, as discussed in Section 4.3.2.2.

### 2.3.3 Multipath Propagation

As a result of interactions with obstructions in the propagation environment, the signal arriving at an R-mode receiver will be a sum of numerous delayed and attenuated copies of the transmitted signal. This is referred to as multipath propagation and can be a major source of measurement error in ranging systems.

There is little information on multipath VHF signal propagation in maritime environments in the open literature. The GLA and the Japan Radio Company (JRC) conducted channel sounding campaigns to characterise the VDES ship-shore channels [14], [15] [16], [17]. Measurement environments included harbours in rural and urban areas, coastal and confined waters, and areas with off-shore infrastructure and open sea. In some types of environment a root-mean-squared (RMS) delay spread in excess of 10  $\mu$ s (3 km) was observed and **multipath propagation is therefore expected to have a significant impact on the achievable R-mode accuracy.**

### 2.3.4 'Additional Secondary Factors'

As mentioned earlier in Section 2.1, researchers from the DMU claim that changing environmental conditions give rise to a significant variability in the propagation delay of VHF signals sent over sea paths. Reference [6] described an 'Additional Secondary Phase Correction System for AIS Signals' developed by the DMU in order to compensate for the environmental factors. The system consisted of a single transmitter and two receivers, one of which was installed in close proximity of the transmitter in order to help calibrate the system. The transmitter and receivers were synchronised using GNSS-disciplined Rubidium clock. The test signal was a Pseudo-Random Number sequence, BPSK-modulated onto a 160 MHz carrier. The receivers used a bank of correlators to accurately estimate the time of flight of the test signals. Some aspects of the system are patented [18].

The paper presented results of several days' worth of 'ASF' measurements performed across a fixed propagation path of approximately 9 km length, over sea water. **Diurnal changes in ASFs of between 1  $\mu$ s and 2.5  $\mu$ s (corresponding to a range difference of 300 m to 750 m) were observed.** Some correlation with environmental factors such as temperature, wind speed, wind direction and cloud cover and time of day was observed.

**Note: As the analysis below suggests, the changes in propagation delay observed by the DMU seem too big to be caused by environmental factors alone; further experiments should be conducted to independently verify these results. It is suggested that the observed delays may also have been caused by multipath propagation whereby a signal arriving at the receiver by the direct path is combined with a delayed signal arriving via higher layers of the troposphere.**

#### 2.3.4.1 Preliminary Analysis of the Effect of Environmental Factors on Propagation Delay

The effect of the propagation medium on the signal propagation speed/delay is commonly modelled using the *refractive index* of the medium, defined by:

$$n = \frac{c}{v},$$

where  $c$  is the speed of light in free space and  $v$  is the propagation speed in the medium.

The refractive index of the air is a function of several environmental factors and can, according to Kerr [19], be modelled using the following expression:

$$n(T, p, e) = 1 + \frac{79 \cdot 10^{-6}}{T} \left( p + \frac{4800e}{T} \right), \quad (1)$$

where  $T$  is the absolute temperature in degrees Kelvin,  $p$  is the atmospheric pressure and  $e$  is the partial pressure of water vapour, both given in millibars.

In order to estimate the maximum likely change in the refractive index (and subsequently propagation delay) in the Dalian region, data on the minimum/maximum temperature,

pressure and humidity in the region was obtained from an online database<sup>3</sup> and is summarised in Table 1.

Temperature (K)		Atmospheric Pressure (mbar)		Relative Humidity		Temperature Relative Humidity Measured at (K)	
$T_{\min}$	$T_{\max}$	$p_{\min}$	$p_{\max}$	$f_{\min}$	$f_{\max}$	$T_{f,\min}$	$T_{f,\max}$
266.15	301.15	1001.6	1030.3	0.50	0.87	287.15	297.15

**Table 1: Environmental data from the Liaoning weather monitoring station, Dalian, China; min/max values over the period of January 2009 to February 2018 are shown.**

Before Equation (1) can be used the minimum and maximum partial pressure of water vapour,  $e_{\min}$  and  $e_{\max}$ , respectively, needs to be calculated from the relative humidity and temperature data provided in Table 1. The partial pressure of water vapour is related to the relative humidity by [19]:

$$e = f \cdot e_s,$$

where  $e_s$  is referred to as the saturation vapour pressure. For a given substance,  $e_s$  is a function of temperature,  $T$ , only; for water vapour,  $e_s$  can be approximated by the following expression [20]:

$$e_s \approx p_s \cdot \exp(13.3185t - 1.9760t^2 - 0.6445t^3 - 0.1299t^4),$$

where  $t = 1 - T_s/T$ ,  $T_s = 373.15$  K and  $p_s = 1013.25$  mbar. The estimated values of  $e_{\min}$  and  $e_{\max}$  for the Dalian region are shown in Table 2.

Partial pressure of water vapour (mbar)	
$e_{\min} = f_{\min} \cdot e_s(T = T_{f,\min})$	$e_{\max} = f_{\max} \cdot e_s(T = T_{f,\max})$
7.99	25.95

**Table 2: Partial pressure of water vapour estimated based on environmental data from the Liaoning weather monitoring station, Dalian, China; min/max values over the period of January 2009 to February 2018 are shown.**

The minimum and maximum expected values of the refractive index,  $n_{\min}$  and  $n_{\max}$ , respectively, can now be calculated by substituting into Equation (1):

$$n_{\min} = n(T_{\max}, p_{\min}, e_{\min}) \approx 1.000296,$$

$$n_{\max} = n(T_{\min}, p_{\max}, e_{\max}) \approx 1.000445.$$

A change in the refractive index,  $\Delta n = n_{\max} - n_{\min}$ , can be related to change in the signal propagation time delay that would be measured over a distance  $r$ , as follows:

$$\Delta\tau = \Delta n \cdot \frac{r}{c}.$$

For the experiments carried out by the DMU,  $r \approx 9000$  m and therefore  $\Delta\tau \approx 4.5$  ns. This figure is two to three orders of magnitude lower than the variation in the 'ASFs' reported by Dalian,

<sup>3</sup> <https://www.worldweatheronline.com/dalian-weather-averages/liaoning/cn.aspx>

suggesting that the variation observed by Dalian may be caused by other mechanisms than just the environmentally-induced changes in the signal propagation speed.

## 2.4 User Equipment Considerations

### 2.4.1 Ranging Algorithms and Theoretical Bounds on Ranging Performance

The ACCSEAS report [1] states that:

'While the AIS transmission has obvious timing characteristics that could be exploited for ranging (carrier phase and times of bit transitions), the complexity of the signal structure and its resulting narrow band nature make the development of effective algorithms difficult. The high frequency AIS carrier can provide sub-meter positioning accuracy; however the ambiguity resolution of the carrier cycle is an issue that must be addressed.'

Cycle ambiguity resolution has not been addressed in any of the subsequent R-mode publications available to the author at the time of writing. **All algorithms for the preferred AIS R-mode architecture proposed to date appear to be based on measuring the time of bit/symbol transition.**

The ACCSEAS report identified several GMSK synchronisation and demodulation algorithms available in the communications literature [21]–[23]. The time of symbol transition (or transmission time delay) is one of the fundamental signal parameters that need to be estimated in any digital communications receiver (although communications receivers may not necessarily be designed to estimate the transmission delay to the level of accuracy desirable for R-mode). The performance of time delay estimators in an Additive White Gaussian Noise (AWGN) channel can be bounded by a Cramér-Rao lower bound, as detailed, for example, in reference [24].

The follow-on report [2] by the ACCSEAS team provided an expanded list of references to GMSK-related literature and established performance bounds for a GMSK transmission time delay estimation in an AWGN channel. Two bounds were provided, one for a message consisting of a random data sequence and one for a fixed, optimal, data sequence, the former resulting in approximately 2 dB worse performance than the latter. Subsequent performance analyses by ACCSEAS used the conservative bound (assuming random message data). **For a 5-slot AIS message, this gave a time delay estimation error of 750 ns, or 225 m (one sigma) at a signal level of -107 dBm (AIS receiver sensitivity level) and 18.8 ns, or 5.7 m (one sigma) at -75 dBm (a typical strong signal).** The report also mentioned that improved performance could be achieved using higher bit-rate transmissions on the VDES channels.

The receivers used in the AAPS system described in the DMU paper [3] estimated the carrier frequency, carrier phase and the time of symbol transition. The paper states that carrier tracking was used in the symbol transition estimation process; however, the description of the symbol transition / time delay estimation algorithm is difficult to follow. The paper states that nearly 200 signal samples were taken in each AIS time slot. These measurements were then averaged to obtain a transmission timing estimate to about 1  $\mu$ s (300 m) accuracy. An alternative estimation algorithm based on Least Squares fitting provided improved accuracy of 0.24  $\mu$ s (73 m). It is not clear whether the stated performance was achieved with noisy signals received over the air (and if so, what the signal to noise ratio was) or based on using "clean", simulated signals.

The DMU paper [4] provided some additional detail on the algorithm used in the AAPS, incl. a Simulink™ block diagram. The paper essentially describes a coherent GMSK demodulator implementation; however, the way of estimating the time delay from the demodulated signal was not described. The paper used the same approach to bounding the time delay estimation error as had been used by ACCSEAS, although the predicted errors stated in the paper seem unrealistically low (3.8 m at a 90 km distance), possibly due to a computation error.

The DMU paper [5] presents two methods of estimating the time delay of AIS signals: the ‘zero-crossing detection’ method and the ‘differential peak detection’ method. Both methods are based on estimating the timing of certain features in a demodulated GMSK signal; however, the details are difficult to follow. The paper also describes an algorithm for combining the measurements obtained by the two methods, termed the ‘alpha difference filter’. The performance of the proposed ranging methods was evaluated both in a computer simulation and experimentally. Results of simulations for an AWGN channel show that the zero-crossing detection method is uniformly better than the differential peak detection method. With a 1250-bit message, a pseudorange error of 100 m and 10 m (one sigma) was achieved for a signal received at a Signal-to-Noise Ratio (SNR) of 10 dB and 30 dB respectively. The paper states that the simulated performance was in line with the modified Cramér-Rao bound established in the ACCSEAS study. Results of the experimental verification are described in Section 2.5.

An important difference between the techniques proposed by the DMU and the ACCSEAS-proposed method is that the ACCSEAS method used dedicated R-mode messages, whereas the DMU method was designed to use ordinary user data messages (and therefore would not increase the AIS data link loading).

#### 2.4.2 Position Calculation and Theoretical Bounds on Positioning Performance

The ACCSEAS report [2] used a ‘weighted HDOP’ approach to bound the positioning errors across the analysis area (North Germany and Denmark). The positioning accuracy plots presented in the report do not take into account any errors due to timing offsets between transmitters (perfect transmitter synchronisation was assumed), nor do they take into account multipath propagation; the only source of measurement error was the radio noise. The assumption was made that 60 slots per minute would be used for ranging (or one 256-bit slot per second) and a receiver averaging time of 5 seconds would be used, for a total of 1280 bits. **The predicted positioning accuracy was around 20 m (presumably 2DRMS) for much of the ACCSEAS analysis area.**

The AAPS system described in the DMU paper [3] used the TDOA (Time Difference of Arrival) positioning method rather than TOA (Time of Arrival)-based positioning. Additional Secondary Factor corrections were also applied, as described in Section 2.3.4. Positioning performance figures are provided in Section 2.5.

The DMU paper [4] presents HDOP and positioning accuracy plots for the North, South and East China Sea regions; however, the positioning accuracy figures cannot be trusted due to the unrealistically low predicted ranging errors (see Section 2.4.1).

#### 2.4.3 Standards Modifications and Limitations of Existing Equipment

For all proposed AIS R-mode architectures, an R-mode receiver would need to be implemented separate from an existing Class-A AIS transceiver on-board. It would not be feasible to modify existing radios to do ranging [2]. However, there is an opportunity to integrate R-mode into the emerging VDES standard.

### 2.5 Experimental Verification

**AIS R-mode field testing has so far been conducted only by the DMU, China [3]–[6].** Available information on the equipment used in these trials was summarised in previous sections. It is not clear from the information available whether existing AIS base stations or purpose-built equipment were used in the trials; however, the latter seems more likely.

Paper [3] describes an experimental setup established in the Xinghai Bay area, Dalian, China. The setup consisted of one Master and two Slave base stations operating in a TDOA fashion. The Master-Slave baselines were approximately 5 km long. An ASF correction system was also set up, as described in Section 2.3.4. **Positioning accuracy of approximately 100 m (2DRMS) was achieved in an area with HDOP < 1.5; it was reported that applying ‘ASF**

**corrections' to the range measurements had resulted in a reduced position error of approximately 9 m (2DRMS).** Both static and dynamic vessel trials were conducted with little difference in performance observed.

Further experimental results obtained using the same system setup were presented in paper [4]. It was reported that position accuracy of 19 m (RMS) and 5 m (RMS) had been obtained in areas with HDOP of 4.5 and 1.2, respectively. It is not clear whether 'ASF corrections' were applied in this case.

Experiments were also conducted in the same area in order to verify the ranging algorithms described in paper [5]. In these experiments, directional Yagi-Uda antennas were used to minimise the effects of multipath propagation. Tests were conducted over ranges of approximately 7 km to 9 km. Ranging precision of 60 m (one sigma) was obtained using one-slot AIS messages and 28 m (one sigma) for five-slot messages. As above, it is not clear whether real-time propagation corrections were used.

### 3 Identification of Gaps and Next Steps

This section provides a summary of open questions identified through the literature review above, and recommends next steps.

#### 3.1 Requirements Capture

At the time of writing, **there is no formal set of user requirements for AIS/VDES R-mode**. A clear set of requirements / goals needs to be defined based on which an optimal system architecture may be derived.

For example, it is not clear whether R-mode needs to operate as a standalone positioning system or only as a component in a multi-system-receiver (MSR) approach, providing one or more (pseudo)range measurements for an integrated position solution.

The performance requirements for R-mode also need to be defined. Are the requirements in Resolutions IMO A.1046/A.915 [25], [26] relevant or would lower performance levels be acceptable?

Does the system have to be completely independent of GNSS? If not, what is the minimum time period over which it must maintain the required performance levels in case of a GNSS outage?

Is it acceptable for the system to be capacity limited? If so, what is the required capacity?

What is the expected cost of equipment and operation?

#### 3.2 System Architecture

A standalone VDES R-mode positioning system can be considered to consist of the following key components:

1. A *VDES Base Station* (BS) transmitting (and possibly receiving) ranging signals to (and from) R-mode user equipment; at least three / two BS are required to support positioning by passive / active ranging, respectively;
2. A *Base Station Synchronisation Subsystem* (BSSS) which ensures that the transmissions from all BS in the system are synchronised to a common time standard;
3. A *Real-time Propagation Correction Subsystem* (RTPCS) may be used in conjunction with the BSSS to measure the changes in signal propagation speed due to changing environmental factors and pass this information on to the BS for transmission to users;
4. A *Base Station Monitoring Subsystem* (BSMS) may be used instead of the BSSS (and RTPCS) if BS synchronisation is not desirable or feasible. The BSMS measures the time of arrival of the signals from the BS at one or more known location(s) in order to estimate the BS clock biases (or relative time-differences between the BS) and passes these on to the BS for transmission to users. To some extent, the BSMS would also compensate for errors due to changing propagation conditions in the vicinity of the monitoring location(s);
5. An *Integrity Monitoring Subsystem* (IMS) which ensures the R-mode signal integrity;
6. *VDES R-mode user equipment* (UE) which receives and processes the ranging signals transmitted by the BS, calculates the user's position, and possibly also transmits ranging signals to support active ranging.

Depending on which of the components are used within the system and how they are configured, a number of candidate R-mode system architectures can be envisaged, as outlined in Table 3.

Architecture	BSSS is required	BSMS is required	UE transmits a ranging signal	UE is equipped with a high-stability clock
Passive Ranging	✓	✗	✗	✗
Passive ranging off unsynchronised transmissions	✗	✓	✗	✗
Active (two-way) Ranging	✗	✗	✓	✗
Passive ranging with high-stability receiver clock initialised by GNSS (when available)	✓	✗	✗	✓
Passive ranging with high-stability receiver clock initialised by active ranging	✓	✗	✓	✓

**Table 3: Example VDES R-mode system architectures.**

Architecture	Pros	Cons
Passive Ranging	Low complexity / cost of UE (UE is receive only); Unlimited system capacity	High cost of BS / BSSS (all BS must be synchronised); At least three BS must be in view to determine position; Off-shore BS likely to be required to achieve good geometry
Passive ranging off unsynchronised transmissions	Relatively low complexity / cost of UE (UE is receive only but needs to be able to decode BS clock bias data from the BSMS); Potentially lower infrastructure costs (BS' do not need to be synchronised)	BSMS reference stations need to be deployed; At least three transmitters must be in view to determine position; Off-shore BS likely to be required to achieve good geometry
Active (two-way) Ranging	Position can be determined using only two BS; BS don't need to be synchronised; Good geometry may be achievable with land-based BS only	High complexity / cost of UE and BS (both UE and BS must be capable of transmitting ranging signals and accurately estimating signal time of arrival); Limited user capacity
Passive ranging with high-stability receiver clock initialised by GNSS (when available)	Position can be determined using only two BS; Unlimited system capacity; Good geometry may be achievable with land-based BS only	Higher cost of UE (UE includes high-stability clock); Performance may degrade after a period of GNSS unavailability
Passive ranging with high-stability receiver clock initialised by active ranging	Position can be determined using only two BS; Performance does not degrade in case of GNSS unavailability; Good geometry may be achievable with land-based BS only	High complexity / cost of UE and BS; Limited capacity (but higher capacity than pure active ranging)

**Table 4: Some pros and cons of the example VDES R-mode system architectures.**

As can be seen from Table 4, each of the candidate architectures has different pros and cons and these would need to be assessed against the (as yet unknown) set of user requirements for R-mode in order to arrive at the optimal architecture.

Other architectural considerations may include:

- Selection of the most appropriate VDES subsystem for R-mode (AIS vs. ASM vs. VDE-TER);
- Need for a real-time 'ASF Correction' system (RTPCS) and / or 'ASF maps';

- Use of signal Direction-of-Arrival (DOA) measurements in addition to / instead of ranging;
- Use of other positioning sensors / systems in conjunction with VDES R-mode.

### 3.3 Base Station Considerations

#### 3.3.1 Signal Structure

Open questions with respect to the R-mode signal structure include:

- Use of dedicated R-mode transmissions vs. ranging off ordinary user data transmissions to minimise VDES data link loading;
- R-mode channel bandwidth (25 kHz, 50 kHz, 100 kHz, any);
- Selection of the optimal modulation scheme;
- The minimum R-mode message rate to satisfy the R-mode performance requirements, and the impact on the VDES data link loading.

#### 3.3.2 Synchronisation

The requirements for a synchronisation source for the candidate R-mode architectures that require BS synchronisation were assessed in the ACCSEAS report [2] (see Section 2.2.2).

Requirements for a base station frequency standard for architectures that do not require synchronisation and requirements for the high-stability receiver clock used within some of the candidate architectures remain to be assessed.

#### 3.3.3 Availability of Base Stations and Station Geometry

In order to be able to accurately model station availability and geometry within a geographical area it is necessary to establish the maximum range at which the R-mode signal can provide sufficient ranging accuracy to meet the user requirements. This subject is addressed in Section 4 of this document.

#### 3.3.4 Standards Modifications and Limitations of Existing Equipment

As explained in Section 2.2.4, in order to enable AIS/VDES R-mode, changes would be required to both the AIS and VDES specifications. Clarification is needed from equipment manufacturers regarding the technical and cost implications of the required changes in specification.

Clarification is also needed from ITU/IALA as to whether a change to the Radio Regulations is required in order to allow the use of the AIS/VDES channels for radionavigation.

### 3.4 Propagation Channel

#### 3.4.1 Multipath Propagation

**The effects of multipath propagation have not been considered in any of the theoretical studies of AIS R-mode published to date**, even though this is expected to be one of the key performance limiting factors for AIS/VDES R-mode. Ranging performance in a multipath fading channel will be investigated in a future report.

#### 3.4.2 Radio Noise / Interference

Only limited data on VHF radio noise and interference on-board maritime vessels is currently available. A measurement campaign may need to be carried out to determine the noise and interference characteristics across a range of vessel types and during different phases of voyage.

#### 3.4.3 'ASFs'

Open questions with respect to the 'ASFs' include:

- Is the signal propagation delay variability observed by the DMU (see Section 2.3.4) reproducible?
- Assuming significant variability is observed, what is the best way of compensating for this effect?
- Spatial and temporal decorrelation of real-time corrections (assuming these are required);
- Are 'ASF maps' required?

### 3.5 User Equipment Considerations

#### 3.5.1 Ranging Algorithms and Theoretical Bounds on Ranging Performance

Performance bounds and references for time delay estimation algorithms that could support AIS R-mode were provided in the ACCSEAS report [2]; some AIS signal processing algorithms were also proposed by the DMU (see Section 2.4.1). Further work in this area is required in order to:

- Establish theoretical bounds on the signal time delay estimation accuracy for the different VDES subsystems, given realistic VHF noise and multipath conditions; this subject is addressed in Section 4 of this document;
- Design an appropriate time delay estimation algorithm for VDES R-mode, noting that a range of different modulation and coding schemes may be used in VDES.

#### 3.5.2 Position Calculation and Theoretical Bounds on Positioning Performance

Positioning algorithms for passive ranging systems and methods of modelling their accuracy are well described in the literature (see e.g. [27]); however, further work may be required in order to:

- Design a suitable positioning algorithm for the active ranging and / or hybrid R-mode architectures (assuming these are considered viable alternatives to passive ranging);
- Establish theoretical performance bounds for the above algorithm(s).

#### 3.5.3 Standards Modifications and Limitation of Existing Equipment

As stated previously, neither the AIS nor the draft VDES standard currently support ranging; however, there is an opportunity to integrate the R-mode capability into the VDES specification being developed by the ITU, IALA and IEC.

Clarification is needed from equipment manufacturers as to whether any changes to the currently considered VDES user equipment architecture are required to support R-mode and what the cost implications would be. It is possible that a passive ranging capability could be implemented on existing prototype VDES units as a software upgrade; implementing active ranging may require some hardware changes in order to reduce the transmission timing jitter.

### 3.6 Experimental Verification

Some experimental work will be necessary in order to answer many of the questions raised in this document, particularly in the following areas:

- AIS/VDES transmission timing jitter and achievable synchronisation accuracy;
- Multipath characteristics of the AIS/VDES propagation channel;
- VHF radio noise / interference levels on maritime vessels;
- Diurnal and seasonal variability of VHF signal propagation delay / speed and the need for real-time corrections;
- Spatial and temporal decorrelation of real-time propagation corrections (if needed);
- Ranging performance in real-world maritime environments (with/without corrections).

### 3.7 Recommended Next Steps – A Development Roadmap

Given the work carried out by the international maritime community to date and the questions identified in the preceding section, it is recommended that future work should:

1. Focus on VDES R-mode rather than AIS R-mode (noting that VDES includes AIS).

Initial investigations suggest that existing AIS base stations cannot be synchronised to the level of accuracy likely to be required for R-mode. Rather than trying to retrofit R-mode to AIS, it seems easier to integrate this capability into the emerging VDES standard.

It has also been reported that AIS networks in some parts of the world are approaching the limits of their capacity; therefore adding further traffic on the AIS channels is not advisable [28].

Finally, VDE transmissions occupy a wider bandwidth than AIS and therefore are expected to provide better ranging performance (as shown in Section 4).

2. Determine the achievable ranging performance under realistic propagation conditions and transmitter-receiver separations.

A good understanding of the factors that limit the ranging accuracy (incl. multipath propagation and changing environmental factors) is necessary in order to be able to determine the optimal R-mode system architecture, model the achievable coverage and positioning performance, and estimate the associated costs.

It is proposed that this activity proceeds in four stages:

- a) Theoretical analysis.

The following tasks are envisaged:

- Propose a channel model – i.e. state assumptions regarding the propagation channel, incl. assumptions on ship's topside noise, multipath, and (if possible) tropospheric delay effects;
- Develop a draft VDES R-mode signal specification;
- Determine theoretical bounds on the ranging performance (such as the Cramér-Rao and Ziv-Zakai bounds), given the channel model and signal structure proposed previously;
- Propose a ranging algorithm for VDES R-mode and carry out computer simulations to compare its performance against the theoretical bounds determined previously.

- b) Measurement system development.

This and the following stages should only be executed if the results of the theoretical analysis indicate VDES R-mode ranging accuracy levels consistent with maritime navigation performance requirements for coastal navigation.

The following tasks are envisaged:

- Design and develop a measurement system implementing the ranging algorithm proposed during the previous stage; this could likely be based on COTS SDR equipment, synchronised using high-quality (e.g. GPS-disciplined Rubidium) clock;
- Develop analysis software to extract basic ranging performance statistics from the measurement data;
- Calibrate and test the measurement system in a laboratory setup.

## c) Measurement campaign.

- Identify suitable measurement locations representing a range of marine environments;
- Develop a Trials Plan;
- Install measurement equipment at the selected locations (and on a ship if required);
- Execute trials, capture data.

## d) Data analysis.

- Analyse data collected during the trials; explore correlations between ranging accuracy and SNR, environment type and weather / sea state conditions.
- Develop / update models for ranging accuracy.

## 3. Define / review the user requirements and consolidate system requirements.

The user requirements for VDES R-mode (and the feasibility of the concept) should be reviewed in light of the findings of the preceding stage(s) and system requirements should be derived.

In particular, this activity should answer the following questions:

- a) Will VDES R-mode operate as a standalone positioning system or as a supporting component in a multi-system approach?
- b) What are the performance requirements for VDES R-mode?
- c) What is the required coverage?
- d) Is it acceptable for R-mode to be capacity limited?

## 4. Propose a system architecture for R-mode.

Given the consolidated set of system requirements, develop a candidate R-mode system architecture.

In particular, this activity should answer the following questions:

- a) What positioning method will be used? Options may include:
  - Passive ranging using three or more base stations;
  - Active (two-way) ranging using two or more base stations;
  - Passive ranging using two or more base stations and a high-stability receiver clock, initialised either by another system (e.g. GNSS when available) or using active VDES ranging.
- b) What VDES subsystem(s) will be used to transmit the ranging signals?
- c) Will additional VDES R-mode stations be deployed or will the transmission network be based on the existing network of AIS base stations?
- d) Will it be possible to deploy VDES R-mode stations offshore?
- e) What type of clock will be used at the base stations?
- f) How will the base station clocks be synchronised?
- g) What type of clock will be used in the user equipment?
- h) Will a real-time propagation correction subsystem be used?

- i) If a multi-system approach is used, what other positioning systems / sensors will R-mode be integrated with?
5. Model the coverage and performance for the proposed system architecture(s) and estimate the cost of the necessary infrastructure, user equipment and operation.
6. Repeat steps 3. to 5. to determine the optimal R-mode system architecture.

The approach proposed above is in line with the recommendations of the UCL report [8]:

'Further research should be conducted to assess the potential of AIS R-mode positioning. This should comprise a hardware demonstrator system that also performs differential ranging using television signals and two-way AIS ranging. Extensive experimental tests should be conducted to determine the ranging performance so that realistic predictions of the position solution accuracy, integrity and availability can be made. The results of this study should be used to generate coverage predictions for a number of possible implementations within the UK and Ireland, together with a cost estimate of the necessary infrastructure.'

## 4 Preliminary Theoretical Analysis of VDES Ranging Performance

This section addresses the first step and first stage of the second step of the VDES R-mode development roadmap proposed in the preceding section.

### 4.1 VDES R-mode Signal Specification

In order to be able to quantify the achievable VDES ranging performance some assumptions regarding the VDES R-mode signal structure must be made. The assumptions made here are largely based on the recommendations of the ACCSEAS AIS R-mode study [2] and the most recent version (as of April 2018) of the VDES Technical Specification [11].

#### 4.1.1 VDES Subsystems and their Suitability for R-mode

The VDES consists of four subsystems, each dedicated to different functions and using different radio waveforms over different radio channels:

1. The *Automatic Identification System* (AIS) uses two 25 kHz simplex channels for ship position reporting and other applications and is considered an integral part of VDES; it has the highest priority within the system and all other subsystems are organised such that the AIS is not adversely affected;
2. Another two 25 kHz simplex channels are dedicated for existing and new IALA and IMO-defined *Application Specific Messages* (ASMs); the ASM subsystem gives a high reliability of message delivery and message acknowledgement support; in addition to the terrestrial component (ASM-TER), ASM also includes a satellite up-link (ASM-SAT);
3. The *terrestrial VHF Data Exchange* (VDE-TER) subsystem comprises a 100 kHz bandwidth duplex channel which is available for data exchange which requires higher capacity than the ASM; the VDE-TER channel can be split into two 50 kHz channels, or four 25 kHz channels; the three possible configurations of the VDE-TER waveform will be referred to here as VDE-TER 100K, VDE-TER 50K, and VDE-TER 25K, respectively;
4. The VDES concept also includes a *satellite component* (VDE-SAT) to enable bidirectional communication in remote areas outside the coverage of shore stations; the spectrum allocation for VDE-SAT will be addressed at the World Radiocommunication Conference in 2019.

This analysis considers the suitability for R-mode of the three terrestrial VDES subsystems (AIS, ASM-TER and VDE-TER). The satellite component is not considered suitable, not least because this would require the position of the VDES satellites to be accurately measured and known to the users at all times.

#### 4.1.2 VDES Modulations

The AIS and VDES technical specifications [9], [11] include four types of modulation, as shown in Table 5. The following sections provide a mathematical description of the modulated signal for each of the modulations shown here.

VDES Subsystem	Modulation
AIS	Gaussian Minimum Shift Keying (GMSK)
ASM-TER	Pi/4 Quaternary Phase Shift Keying (Pi/4-QPSK)
VDE-TER	Pi/4-QPSK 8-state Phase Shift Keying (8-PSK) 16-state Quadrature Amplitude Modulation (16-QAM)

**Table 5: VDES modulations.**

#### 4.1.2.1 GMSK

The GMSK modulation used in AIS belongs to the family of *Continuous Phase Modulations* (CPM). A CPM-modulated signal can be written as follows<sup>4</sup> [29]:

$$s(t) = \sqrt{\frac{2E_s}{T_s}} e^{j\phi(t, \mathbf{d})},$$

where  $\mathbf{d} = \{d_n\}_{n \in \mathbb{Z}}$  is a vector of *data symbols* from the alphabet  $\{\pm 1, \pm 3, \dots, \pm(M-1)\}$ ,  $E_s$  is the average energy per symbol of the real modulated signal,  $T_s$  is the symbol period,  $j = \sqrt{-1}$  is the imaginary unit, and  $\phi(t, \mathbf{d})$  is the instantaneous phase:

$$\phi(t, \mathbf{d}) = 2\pi\kappa \sum_n d_n \beta(t - nT_s).$$

The parameter  $\kappa$  in the above equation is commonly referred to as the *modulation index*.  $\beta(t)$  is the *phase response* of the modulator, which is related to its *frequency response*,  $\mu(t)$ , by:

$$\beta(t) = \int_{-\infty}^t \mu(s) ds.$$

For GMSK,  $M = 2$ ,  $\kappa = 1/2$  and the frequency response is obtained as a convolution of a rectangular pulse and a Gaussian-shaped pulse (hence the name of the modulation); the frequency response is given by the following expression [2]:

$$\mu(t) = \frac{Q\left(\frac{2\pi B}{\sqrt{\ln 2}}\left(t - \frac{L+1}{2}T_s\right)\right) - Q\left(\frac{2\pi B}{\sqrt{\ln 2}}\left(t - \frac{L-1}{2}T_s\right)\right)}{2T_s},$$

where  $B$  (bandwidth parameter) and  $L$  (correlation length) are system design parameters and  $Q(x)$  is the complementary cumulative distribution function of the standard Gaussian distribution:

$$Q(x) = \frac{1}{\sqrt{2\pi}} \int_x^{\infty} e^{-y^2/2} dy.$$

The AIS specification [9] requires that  $BT_s = 0.4$ ; however, it doesn't seem to state any requirements on the correlation length,  $L$ . Reference [2] states that, for GMSK, typically  $L = 4$  or 5; therefore  $L = 4$  will be assumed in this document.

<sup>4</sup> Unless otherwise stated, this analysis uses the complex envelope representation of radio signals.

#### 4.1.2.2 PSK/QAM

The Pi/4-QPSK, 8-PSK and 16-QAM modulations used in VDES all belong to the class of linear modulations; therefore, the modulated signal has the form:

$$s(t) = \sum_n q_n h(t - nT_s),$$

where  $q_n$  are complex-valued *channel symbols* and  $h(t)$  is a suitable *modulation pulse*, as discussed further below.

In the case of the Pi/4-QPSK modulation, the channel symbols can be determined from the data symbols,  $d_n$ , and internal states of the modulator,  $\sigma_n$ , as follows:

$$q_n = d_n e^{j\frac{\pi}{4}\sigma_n},$$

$$\sigma_n = \begin{cases} 1, & n = 0 \\ ((\sigma_{n-1} + 1) \bmod 2), & n > 0 \end{cases}$$

where  $a \bmod b$  denotes the remainder of  $a$  after division by  $b$ . The data symbols are taken from the alphabet:

$$d_n \in \left\{ e^{j\frac{\pi}{2}i} \right\}_{i=0}^3,$$

and consequently, the channel symbol alphabet (also referred to here as *constellation*) has the following eight members:

$$q_n \in \left\{ e^{j\frac{\pi}{4}i} \right\}_{i=0}^7.$$

In other words, the channel symbols are alternately drawn from two QPSK constellations, rotated with respect to each other by  $\pi/4$  rad (which gives the modulation its name). This arrangement reduces the peak-to-average power ratio of the modulated signal by ensuring that its envelope never collapses to zero. This increases the robustness of the waveform against non-linear distortion introduced by transmitter power amplifiers.

For 8-PSK, the channel symbols are the same as the data symbols and are given by:

$$d_n \in \left\{ e^{j\frac{\pi}{4}i} \right\}_{i=0}^7,$$

$$q_n = d_n,$$

For 16-QAM, the symbols are given by:

$$d_n \in \{(2i_1 - 5) + j(2i_2 - 5)\}_{i_1=1, i_2=1}^{4,4},$$

$$q_n = d_n.$$

Arguably the most common modulation pulse,  $h(t)$ , used in digital communication systems is the *Root-Raised Cosine* (RRC) pulse, which is defined in the frequency domain as follows<sup>5</sup>:

$$H(f) = \mathcal{F}\{h(t)\} = \begin{cases} \sqrt{T_s}, & |f| < \frac{1-\alpha}{2T_s} \\ \sqrt{T_s} \cos\left(\frac{\pi T_s}{2\alpha} \left(|f| - \frac{1-\alpha}{2T_s}\right)\right), & \frac{1-\alpha}{2T_s} \leq |f| < \frac{1+\alpha}{2T_s} \\ 0, & \frac{1+\alpha}{2T_s} \leq |f| \end{cases}$$

The coefficient  $\alpha$ ,  $0 < \alpha < 1$ , is referred to as the *roll-off factor* and is a measure of the excess bandwidth, i.e. the bandwidth occupied by the modulated signal beyond the Nyquist bandwidth

<sup>5</sup>  $\mathcal{F}\{h(t)\}$  denotes the Fourier transform of  $h(t)$ .

of  $1/(2T_S)$ . The VDES specification [11] does not explicitly specify the type of the modulation pulse; however it does specify the roll-off factors for the different modulations, implying the RRC pulse should be used. The values of  $\alpha$  stated in the specification (and used in this document) are summarised in Table 6.

VDES Subsystem	Modulation	RRC Roll-off Factor, $\alpha$
ASM-TER	Pi/4-QPSK	0.35
VDE-TER	Pi/4-QPSK	0.30
	8-PSK	0.30
	16-QAM	0.30

**Table 6: RRC roll-off factor values used in VDES.**

As will become clear later, the two variants of PSK and the QAM modulation are equivalent as far as the ranging performance is concerned; therefore these modulations will be treated in the following sections as one case (referred to as 'PSK/QAM').

#### 4.1.3 Symbol Rate

The *symbol rate* (also referred to as Baud rate),  $R_S$ , is related to the symbol interval by:  $R_S = 1/T_S$ . As will be seen later, the symbol rate is one of the key factors determining the achievable ranging performance, with higher symbol rates promising improved ranging accuracy. The values of  $R_S$  used in VDES are summarised in Table 7.

VDES Waveform Configuration	Symbol Rate (symbols/s)
AIS	9,600
ASM-TER	9,600
VDE-TER 25K	19,200
VDE-TER 50K	38,400
VDE-TER 100K	76,800

**Table 7: Symbol rates for different VDES waveform configurations.**

#### 4.1.4 Transmission Duration and Number of Symbols used for Range Estimation

The number of VDES symbols used in the range estimation process is another important parameter that affects the achievable ranging performance. The VDES uses the same TDMA frame structure as the AIS, with 2,250 time slots per minute; however, the VDES specification sets different limits to the maximum duration of transmissions for different VDES subsystems. In addition, a certain number of symbols in a transmission are reserved for the transmitter ramp-up/down and as a guard interval to account for propagation delays; therefore these symbols cannot be used for ranging.

Table 8 shows two potential VDES R-mode transmission configurations that will be considered in this document:

1. *One-slot Bursts* – range estimates are made based on R-mode transmissions occupying one VDES time-slot;
2. *Maximum-length Bursts* – R-mode uses the maximum transmission duration allowed by the VDES specification [11]; note from Table 8 that different VDES subsystems have different maximum transmission durations.

For each configuration, Table 8 shows the number of time slots occupied by an R-mode transmission and the corresponding number of symbols that are potentially available for range estimation.

VDES Waveform Configuration	One-slot Bursts		Maximum-length Bursts	
	Number of Slots	Number of Symbols per Observation, $L_o$	Number of Slots	Number of Symbols per Observation, $L_o$
AIS	1	224	5	1,248
ASM-TER	1	240	3	752
VDE-TER 25K	1	480	1	480
VDE-TER 50K	1	960	1	960
VDE-TER 100K	1	1,920	1	1,920

**Table 8: Potential VDES R-mode transmission configurations.**

#### 4.1.5 Data Sequence

There appear to be two options with regards to the data sequence transmitted by VDES R-mode stations:

1. R-mode base-stations transmit an agreed, fixed, sequence of symbols. The advantage of this approach, apart from implementation simplicity, is that the sequence could be optimised to provide the best ranging performance. A disadvantage is that dedicated time slots would have to be reserved for R-mode transmissions, adding to the VDES data link loading.
2. Another option is that R-mode will use ordinary user data transmissions for ranging. The obvious advantage of this approach is that R-mode would not add to the VDES data link loading. The disadvantages are that the data sequence could not be optimised, the receiver implementation would be more complex than if a fixed sequence was used, and the user would likely need to be located within the data coverage area of the R-mode base station (as the receiver would need to be able to demodulate the user data to enable accurate ranging).

For the purpose of the analysis in this document, it will be assumed that option 2 above is used. No effort will be made here to establish the optimal data sequence that would provide the highest ranging accuracy if option 1 was used.

Further, it will be assumed that the data symbols can be modelled as zero-mean mutually uncorrelated random variables (this is a standard assumption made in digital communications and should be satisfied in any well-designed digital communications system)<sup>6</sup>:

<sup>6</sup> A star, \*, denotes the complex conjugate.

$$\begin{aligned} E\{d_n\} &= 0, \\ E\{d_n d_m^*\} &= \begin{cases} E\{|d_n|^2\} \equiv D, & n = m \\ 0, & n \neq m. \end{cases} \end{aligned}$$

It is easy to show that under these assumptions the channel symbols for the linear modulations defined in Section 4.1.2.2 also are zero-mean and uncorrelated:

$$\begin{aligned} E\{q_n\} &= 0, \\ E\{q_n q_m^*\} &= \begin{cases} E\{|q_n|^2\} \equiv D, & n = m \\ 0, & n \neq m. \end{cases} \end{aligned}$$

## 4.2 VDES Propagation Channel Model

This document establishes bounds on the VDES ranging performance in an Additive White Gaussian Noise (AWGN) channel; accordingly, the received signal is modelled as:

$$r(t) = s(t - \tau) + w(t),$$

where  $s(t)$  is the modulated baseband signal as defined in the preceding section,  $\tau$  is an unknown propagation delay (the quantity of interest for ranging) and  $w(t)$  is a complex white Gaussian noise process with a power spectral density of  $2N_0$  (representing real white Gaussian noise with a two-sided power spectral density of  $N_0/2$ ).

Note: in practice, the received signal will also have an unknown carrier frequency and phase offset (due to a mismatch between the transmitter and receiver oscillators and receiver motion). It can be shown that these offsets have no impact on the performance bounds derived in this document and are therefore omitted for clarity.

Real-world VDES R-mode performance is also likely to be affected by multipath propagation. The achievable performance in a maritime multipath fading channel will be investigated in a future report.

## 4.3 Bounds on Ranging Performance

The ranging accuracy is directly related to the accuracy of estimating the signal propagation delay,  $\tau$ . Estimation theory offers several methods of establishing bounds to the achievable accuracy of signal parameter estimators. Perhaps the most widely used of these methods is the *Cramér-Rao Bound* (CRB) which provides a lower bound to the variance of *any* unbiased<sup>7</sup> estimator [24]. The CRB can easily be applied to the problem of estimating the delay of a deterministic signal waveform in AWGN. However, its application to practical estimation problems is often complicated by the presence of random nuisance parameters<sup>8</sup>, such as the data symbols in a modulated signal.

A simplified version of the CRB, referred to as the *Modified Cramer-Rao Bound* (MCRB), was introduced in reference [24]. The MCRB provides a lower bound to the CRB and can readily be evaluated even in the presence of random nuisance parameters. It can be shown that the MCRB coincides with the CRB when the nuisance parameters are perfectly known (this case corresponds to using a fixed data sequence in the R-mode transmissions). The MCRB was previously used in study [2] to evaluate the ranging performance of AIS R-mode and will therefore serve as the starting point for the current analysis.

<sup>7</sup> An estimator is said to be *unbiased* if, on average, it attains the true value of the parameter being estimated.

<sup>8</sup> In estimation theory, a *nuisance parameter* is any parameter which is not of immediate interest but which must be accounted for in the analysis of those parameters which are of interest.

### 4.3.1 Modified Cramér-Rao Bound for AIS/VDES R-mode

The MCRB for signal delay estimation in AWGN has the form [24]:

$$\text{var}\{\hat{\tau}\} = \frac{N_0}{E_d \left\{ \int_0^{T_0} \left| \frac{\partial s(t, \tau, \mathbf{d})}{\partial \tau} \right|^2 dt \right\}}, \quad (2)$$

where  $\hat{\tau}$  is the estimate of the true signal delay  $\tau$ ,  $T_0$  is the observation interval over which the estimation is performed, and  $E_d\{\cdot\}$  denotes statistical expectation with respect to the data symbols,  $\mathbf{d}$ . The bound will now be applied first to the AIS and then the VDES waveforms.

#### 4.3.1.1 GMSK (AIS)

For a GMSK signal (see Section 4.1.2.1), the denominator in the MCRB expression above can be written as:

$$\begin{aligned} E_d \left\{ \int_0^{T_0} \left| \frac{\partial}{\partial \tau} \sqrt{\frac{2E_S}{T_S}} e^{j\phi(t-\tau, \mathbf{d})} \right|^2 dt \right\} &= E_d \left\{ \int_0^{T_0} \left| \frac{\partial}{\partial \tau} \sqrt{\frac{2E_S}{T_S}} e^{j\pi \sum_n d_n \beta(t-\tau-nT_S)} \right|^2 dt \right\} \\ &= \frac{2E_S}{T_S} E_d \left\{ \int_0^{T_0} \left| e^{j\pi \sum_n d_n \beta(t-\tau-nT_S)} \cdot j\pi \sum_n d_n \mu(t-\tau-nT_S) \right|^2 dt \right\} \\ &= \frac{2\pi^2 E_S}{T_S} \int_0^{T_0} E_d \left\{ \left| \sum_n d_n \mu(t-\tau-nT_S) \right|^2 \right\} dt, \end{aligned}$$

where  $\mu(t) = \frac{\partial \beta}{\partial t}$  is the GMSK frequency response, as defined in Section 4.1.2.1.

Using the assumption of uncorrelated data symbols (see Section 4.1.5), the linearity of expectation and the fact that, for GMSK,  $E\{|d_n|^2\} = 1$ , the expression above can be simplified to:

$$\frac{2\pi^2 E_S}{T_S} \int_0^{T_0} \sum_n \mu^2(t-\tau-nT_S) dt.$$

Further, by using the Poisson summation formula [30] and assuming that the observation interval,  $T_0$ , is an integer multiple of the symbol interval,  $T_0 = L_0 T_S$ ,  $L_0 \in \mathbb{N}$ , the expression can be rewritten as:

$$\frac{2\pi^2 E_S L_0}{T_S} \underbrace{\int_{-\infty}^{\infty} \mu^2(t) dt}_{\xi}.$$

By substituting into Equation (2), the MCRB can now be expressed as:

$$\text{var}\{\hat{\tau}\} = \frac{T_S}{2\pi^2 \xi L_0 \frac{E_S}{N_0}}.$$

Note: this result is a factor of 2 smaller than the expression presented in the ACCSEAS AIS R-mode study [2]. The reason seems to be that the ACCSEAS study modelled the modulated signal as a real signal (centred on an RF carrier), instead of using the complex envelope representation assumed by the MCRB expression given by Equation (2).

The variance of the pseudorange<sup>9</sup> estimation error is then given by:

$$\text{var}\{\hat{\rho}\} = c^2 \cdot \text{var}\{\hat{t}\} = \frac{c^2 T_S}{2\pi^2 \xi L_o \frac{E_S}{N_0}},$$

where  $c$  is the signal propagation speed (assumed to be equal to the speed of light in free space in this document).

Denoting  $\eta_{\text{GMSK}} \equiv \frac{c^2 T_S}{2\pi^2 \xi}$ , the expression above can be rewritten as:

$$\text{var}\{\hat{\rho}\} = \frac{\eta_{\text{GMSK}}}{L_o \frac{E_S}{N_0}}.$$

The standard deviation of the pseudorange estimation error is then given by:

$$\sigma_{\hat{\rho}, \text{GMSK}} = \sqrt{\text{var}\{\hat{\rho}\}} = \sqrt{\frac{\eta_{\text{GMSK}}}{L_o \frac{E_S}{N_0}}}.$$

Alternatively, the bound can be expressed in terms of the carrier-power-to-noise-density ratio,  $C/N_0$ , using the identity  $E_S = CT_S$ , where  $C$  is the carrier power (equal to the average power of the real modulated signal):

$$\sigma_{\hat{\rho}, \text{GMSK}} = \sqrt{\frac{\eta'_{\text{GMSK}}}{L_o \frac{C}{N_0}}}.$$

For the AIS waveform as defined in Section 4.1.2.1,  $\eta_{\text{GMSK}}$  is found to be equal to  $3.13 \cdot 10^8 \text{ m}^2$  and  $\eta'_{\text{GMSK}} = 3.00 \cdot 10^{12} \text{ m}^2/\text{s}$ . Suitable values for  $L_o$  were provided in Table 8, Section 4.1.4.

As may be intuitively expected, the ranging error decreases with increasing number of data symbols used in the R-mode transmission and increasing SNR.

#### 4.3.1.2 PSK/QAM (VDES)

For a PSK or QAM signal (as defined in Section 4.1.2.2), the denominator in Equation (2) can be written as:

$$\mathbb{E}_{\mathbf{d}} \left\{ \int_0^{T_0} \left| \frac{\partial}{\partial \tau} \sum_n q_n h(t - \tau - nT_S) \right|^2 dt \right\} = \int_0^{T_0} \mathbb{E}_{\mathbf{d}} \left\{ \left| \sum_n q_n p(t - \tau - nT_S) \right|^2 \right\} dt$$

where  $p(t) \equiv \frac{dh(t)}{dt}$ .

Using the assumption of uncorrelated data/channel symbols (see Section 2.1.5) and the linearity of expectation, the expression above can be simplified to:

$$\int_0^{T_0} D \sum_n p^2(t - \tau - nT_S) dt,$$

where  $D \equiv \mathbb{E}\{|d_n|^2\}$ .

---

<sup>9</sup> The term *pseudorange* rather than 'range' is used as, in general, the measurement will be affected by the receiver clock bias which is unknown a priori and needs to be obtained as part of the position solution or by other means.

By using the Poisson summation formula [30] and assuming that the observation interval,  $T_0$ , is an integer multiple of the symbol interval,  $T_0 = L_0 T_S$ ,  $L_0 \in \mathbb{N}$ , the expression can be simplified to:

$$DL_0 P_2(0),$$

where  $P_2(f) \equiv \mathcal{F}\{p^2(t)\}$ . Using the following identities:

$$\mathcal{F}\{p^2(t)\} = \int_{-\infty}^{\infty} P(u)P(f-u) du,$$

in which  $P(f) \equiv \mathcal{F}\{p(t)\}$ , and:

$$P(f) = \mathcal{F}\left\{\frac{dh(t)}{dt}\right\} = j2\pi f H(f),$$

where  $H(f) \equiv \mathcal{F}\{h(t)\}$ , and considering that  $h(t) \in \mathbb{R}$  and therefore  $H(-f) = H^*(f)$ , the Fourier transform  $P_2(0)$  can be expressed as:

$$P_2(0) = \mathcal{F}\{p^2(t)\}|_{f=0} = \int_{-\infty}^{\infty} \left(\frac{dh(t)}{dt}\right)^2 dt = 4\pi^2 \int_{-\infty}^{\infty} f^2 |H(f)|^2 df.$$

Substituting for  $P_2(0)$  in the expression for the denominator gives:

$$DL_0 4\pi^2 \int_{-\infty}^{\infty} f^2 |H(f)|^2 df.$$

For further analysis, it is desirable to express the MCRB in terms of the SNR. It can be shown that the average energy per symbol of the linear modulations defined in Section 4.1.2.2, under the assumptions made in Section 4.1.5, is given by [24]:

$$E_S = \frac{D}{2} \int_{-\infty}^{\infty} |H(f)|^2 df.$$

The expression for the denominator can therefore be rewritten as follows:

$$8\pi^2 L_0 E_S \frac{\int_{-\infty}^{\infty} f^2 |H(f)|^2 df}{\int_{-\infty}^{\infty} |H(f)|^2 df} = \frac{8\pi^2 L_0 E_S \zeta}{T_S^2},$$

where

$$\zeta \equiv T_S^2 \frac{\int_{-\infty}^{\infty} f^2 |H(f)|^2 df}{\int_{-\infty}^{\infty} |H(f)|^2 df}$$

is a dimensionless factor related to the shape of the modulation pulse. For an RRC modulation impulse with a roll-off factor  $\alpha$  (see Section 4.1.2.2),  $\zeta$  can be shown to be equal to [24]:

$$\zeta = \frac{1}{12} + \alpha^2 \left( \frac{1}{4} - \frac{2}{\pi^2} \right).$$

By substituting into Equation (2), the MCRB can then be expressed as:

$$\text{var}\{\hat{t}\} = \frac{T_S^2}{8\pi^2 \zeta L_0 \frac{E_S}{N_0}}.$$

The variance of the pseudorange estimation error is given by:

$$\text{var}\{\hat{\rho}\} = c^2 \cdot \text{var}\{\hat{t}\} = \frac{c^2 T_S^2}{8\pi^2 \zeta L_0 \frac{E_S}{N_0}}.$$

Denoting  $\eta_{\text{PSK-QAM}} \equiv \frac{c^2 T_S^2}{8\pi^2 \zeta}$ , the expression can be rewritten as:

$$\text{var}\{\hat{\rho}\} = \frac{\eta_{\text{PSK-QAM}}}{L_o \frac{E_S}{N_0}}.$$

Finally, the standard deviation of the pseudorange estimation error is given by:

$$\sigma_{\hat{\rho}, \text{PSK-QAM}} = \sqrt{\text{var}\{\hat{\rho}\}} = \sqrt{\frac{\eta_{\text{PSK-QAM}}}{L_o \frac{E_S}{N_0}}}.$$

Alternatively, the bound can be expressed in terms of the carrier-power-to-noise-density ratio,  $C/N_0$ , using the identity  $E_S = CT_S$ , where  $C$  is the carrier power:

$$\sigma_{\hat{\rho}, \text{PSK-QAM}} = \sqrt{\frac{\eta'_{\text{PSK-QAM}}}{L_o \frac{C}{N_0}}}.$$

The values of  $\eta_{\text{PSK-QAM}}$  and  $\eta'_{\text{PSK-QAM}}$  for the different modulations and symbol rates used in VDES are provided in Table 9. Suitable values for  $L_o$  were provided in Table 8, Section 4.1.4.

VDES Waveform Configuration	$\eta_{\text{PSK-QAM}}$ (m <sup>2</sup> )	$\eta'_{\text{PSK-QAM}}$ (m <sup>2</sup> /s)
ASM-TER	$1.39 \cdot 10^8$	$1.33 \cdot 10^{12}$
VDE-TER 25K	$3.53 \cdot 10^7$	$6.77 \cdot 10^{11}$
VDE-TER 50K	$8.81 \cdot 10^6$	$3.38 \cdot 10^{11}$
VDE-TER 100K	$2.20 \cdot 10^6$	$1.69 \cdot 10^{11}$

**Table 9: Ranging error coefficients for different VDES waveform configurations.**

#### 4.3.1.3 GMSK (AIS) vs. PSK/QAM (VDES) Comparison

By comparing the values of  $\eta'_{\text{PSK-QAM}}$  in Table 9, Section 4.3.1.2, with the value of  $\eta'_{\text{GMSK}}$  determined in Section 4.3.1.1, it can be seen that all of **the new VDES waveforms can be expected to provide better ranging performance in AWGN than the AIS waveform**. It can also be seen from the table that the **performance improves with increasing waveform bandwidth**. The best performance is achieved using the 100 kHz bandwidth VDES waveforms which provide approximately twelve times better ranging precision than the AIS (assuming the same observation interval length,  $L_o T_S$ , is used).

As may be expected, the ranging performance also improves with increasing signal-to-noise ratio, as illustrated in Figure 2 for one-slot transmissions and in Figure 3 for maximum-length transmissions.

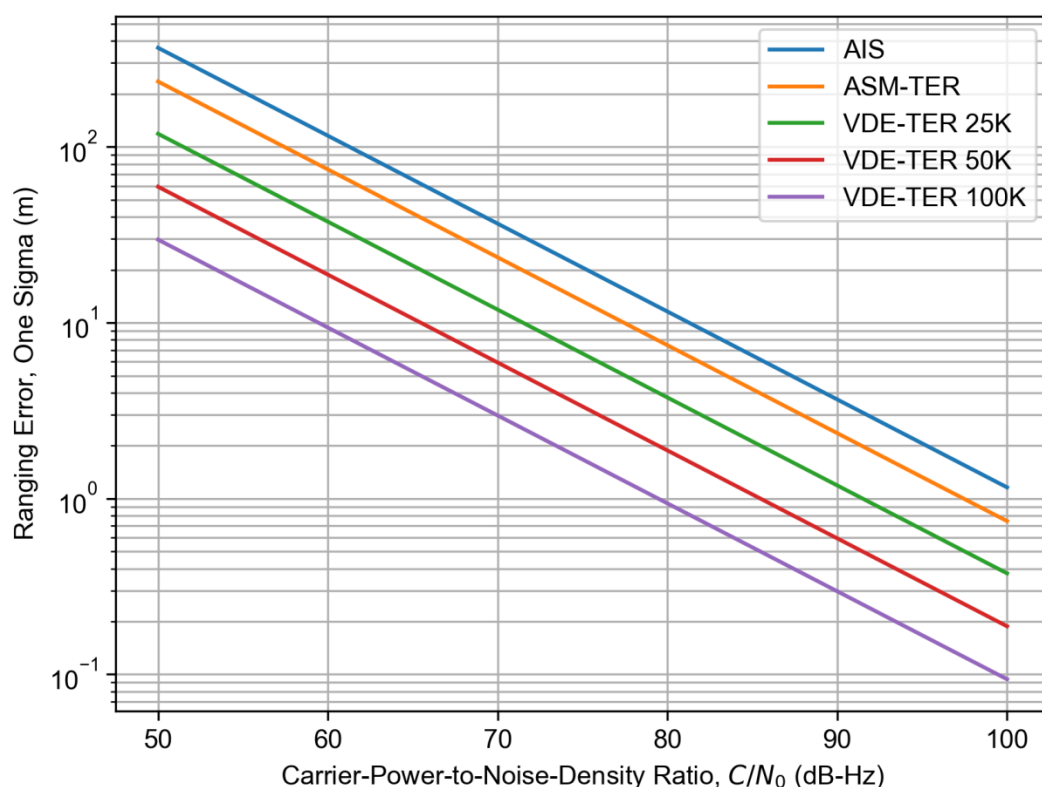


**Figure 2: AIS/VDES ranging error vs. carrier-power-to-noise-density ratio assuming one-slot transmissions.**

#### 4.3.1.4 Receiver Integration

A further improvement in performance could be obtained by combining several successive R-mode transmissions at the receiver end. Different combination methods may be considered and these will be discussed in a later report. Options may include coherent integration of the received bursts, or some form of filtering of the range measurements. The coherent integration would be expected to provide the highest processing gain but would either require the transmitter to maintain carrier phase coherence between the successive R-mode transmissions that are integrated over, or the receiver would have to estimate and compensate for the carrier phase offset on a per transmission basis.

For illustration Figure 4 shows the achievable ranging performance when five successive one-slot R-mode transmissions are coherently combined in the receiver (see also Table 10); as expected based on the MCRBs derived earlier, increasing the number of symbols per observation by a factor of five results in the ranging error being reduced by a factor of  $\sqrt{5} \approx 2.2$ .

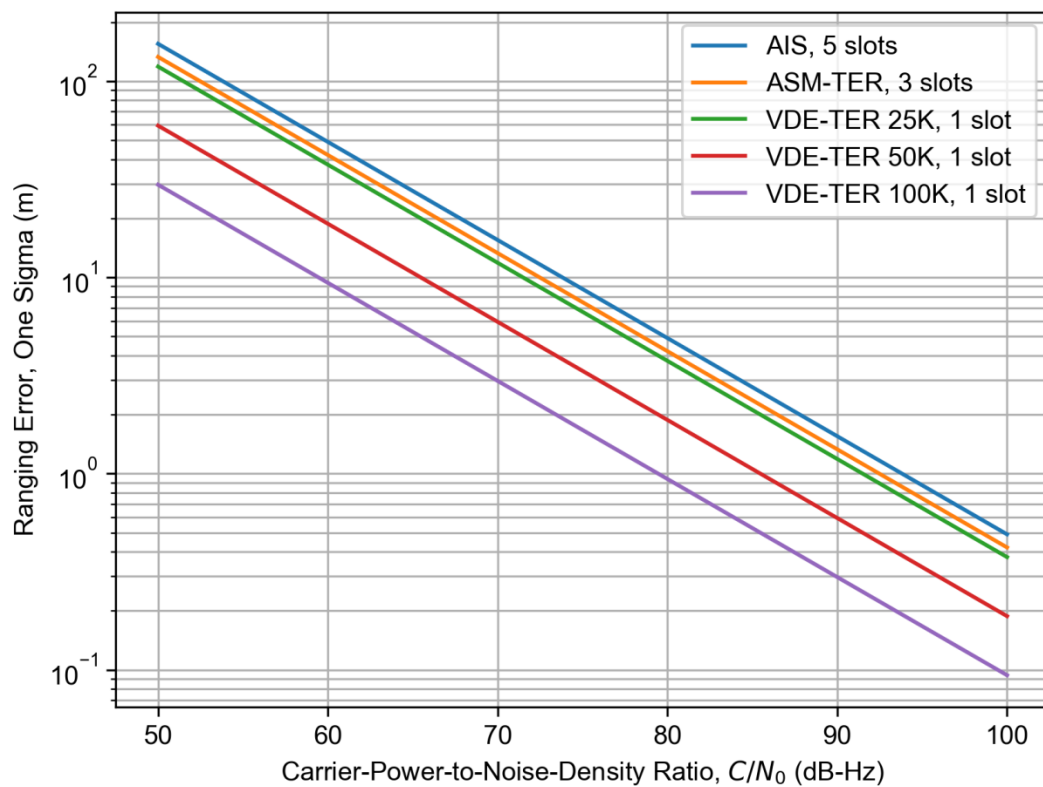


**Figure 3: AIS/VDES ranging error vs. carrier-power-to-noise-density ratio assuming maximum-length transmissions.**

	One-slot Bursts with Receiver Integration	
VDES Waveform Configuration	Number of Slots Integrated over	Number of Symbols per Observation, $L_o$
AIS	5	1,120
ASM-TER	5	1,200
VDE-TER 25K	5	2,400
VDE-TER 50K	5	4,800
VDE-TER 100K	5	9,600

**Table 10: Number of symbols per observation for the one-slot burst transmission configuration with receiver integration.**

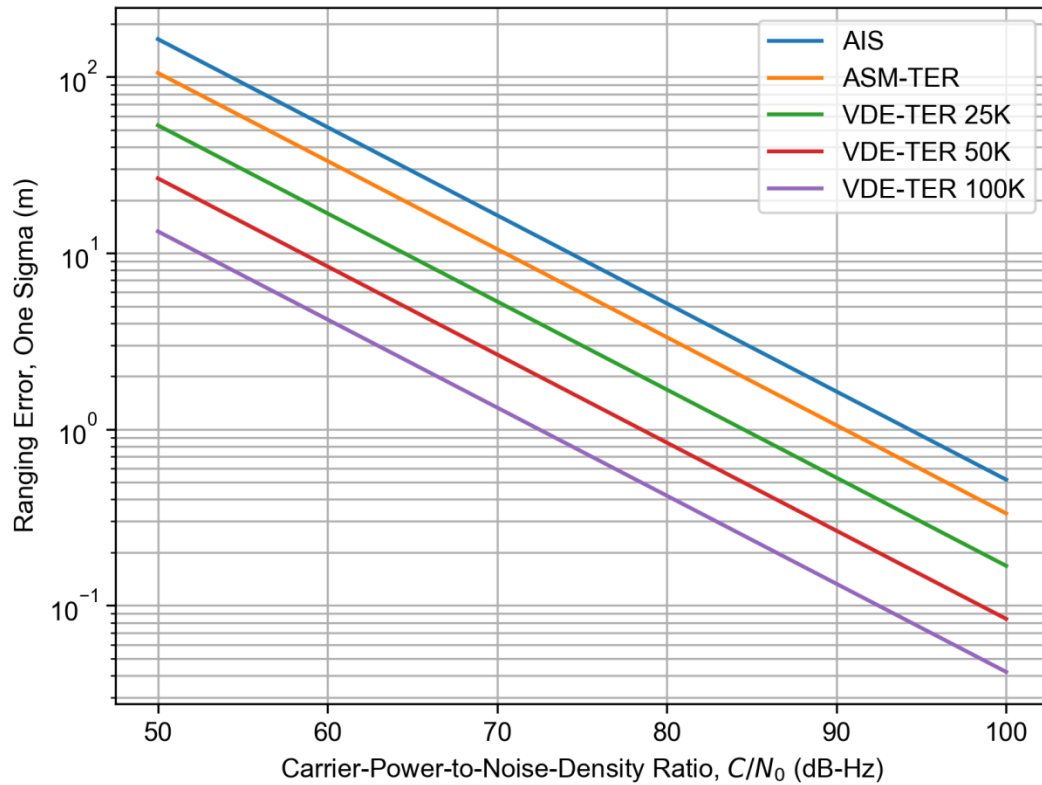


**Figure 4: AIS / VDES ranging error vs. carrier-power-to-noise-density ratio assuming one-slot transmissions and receiver integration over five slots.**

#### 4.3.2 Ranging Performance vs. Distance

In order to relate the performance characteristics derived in the preceding section to distance from the R-mode base station, it is necessary to model the received signal power vs. distance and estimate the radio noise levels likely to be present on maritime vessels. This section does just that.

##### 4.3.2.1 Received Power vs. Distance

The average received signal power at a given distance from the base station, equivalent to the carrier power  $C$  used in the preceding section, can be modelled as follows (all quantities are expressed using a logarithmic scale):

$$C = P_{TX} - L_{t,TX} + G_{TX} - L_B(d, h_{TX}, h_{RX}, \dots) + D_{RX}.$$

In the above equation,  $P_{TX}$  is the base station transmitter output power,  $L_{t,TX}$  represents the transmission line loss incurred at the transmitter,  $G_{TX}$  is the transmitting antenna gain,  $D_{RX}$  is the receiving antenna directivity (i.e. the gain plus the antenna circuit loss), and  $L_B$  is the basic path loss which is a function of the transmitter-receiver distance,  $d$ , antenna heights above the sea level  $h_{TX}$ ,  $h_{RX}$ , and other factors.

There are multiple path loss models for the VHF band available in the literature, some of which had previously been implemented by R&RNAV. In this study, the method described in Recommendation ITU-R P.1546-5 [12] is used to estimate the path loss for an all-sea water path, free of obstructions. This method is based on interpolation/extrapolation from a set of empirically derived field strength curves as functions of distance, transmitting antenna height,

operating frequency, propagation environment type and percentage time for which the stated signal strength is exceeded. The estimated field strength values are then corrected for the height of the receiving antenna and converted to path loss.

A summary of assumptions made when modelling the VDES signal strength is provided in Table 11.

Parameter	Value	Notes
Transmitter output power, $P_{TX}$	41.0 dBm (12.5 W)	Nominal high-power setting for a VDES unit.
Transmitting antenna height above sea level, $h_{TX}$	Two values considered: 18 m; 57 m	Based on AIS antenna installations on the roof of the Trinity House office building in Harwich, UK, and at the North Foreland Lighthouse, respectively.
Receiving antenna height above sea level, $h_{RX}$	10 m	Based on the AIS antenna installation on THV Alert.
Transmitter transmission line loss, $L_{t,TX}$	1.2 dB	Loss in the antenna feeder; based on measurements on a typical GLA' AIS station installation.
Transmitting / receiving antenna gain, $G_{TX}$ , $G_{RX}$	2.15 dBi	Half-wave dipole. Antenna circuit loss is assumed to be negligible.
Basic path loss, $L_B$	Function of the transmitter-receiver distance and other factors.	Calculated according to Rec. ITU-R P.1546-5.
Centre frequency, $f_c$	162 MHz	Approx. centre of the upper VDES band (by default used for shore-to-ship transmissions).
Propagation environment type	Cold sea path	e.g. North Sea
Percentage time power exceeded	50%	
Terrain elevation data	None	Sea water path with no obstructions is assumed.

**Table 11: Assumptions related to received power modelling.**

For illustration, Figure 5 shows the predicted received power as a function of distance for the two representative transmitting antenna heights given in Table 11.

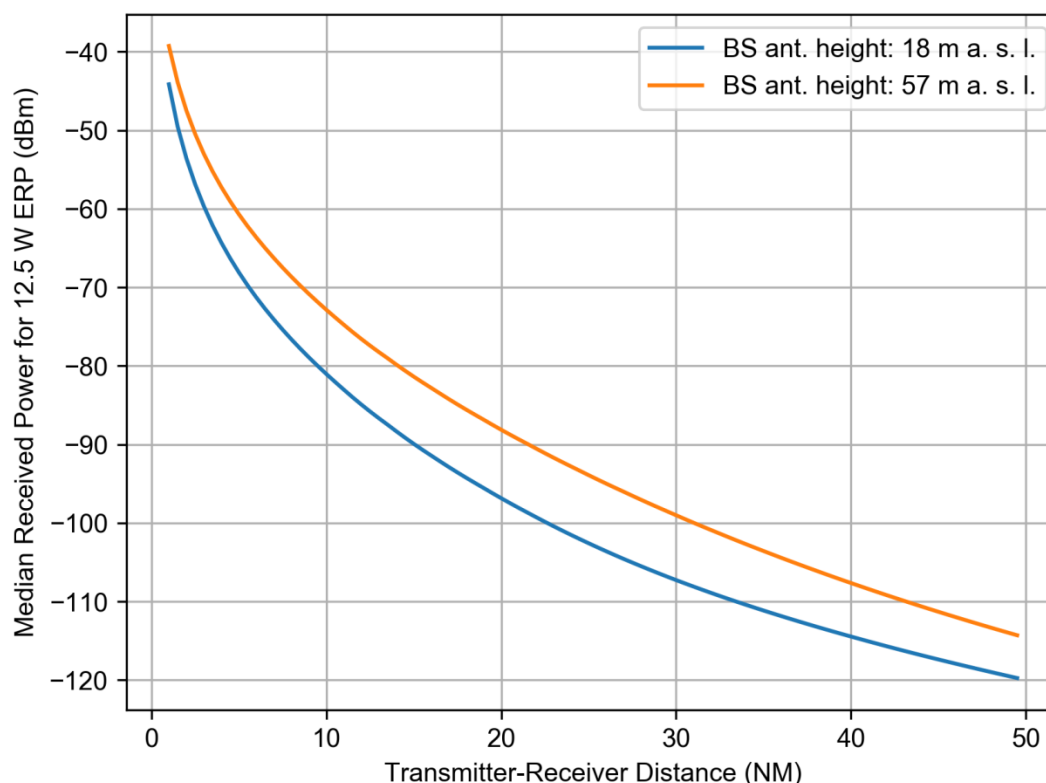


**Figure 5: Received power vs. distance for a 12.5 W ERP VHF transmission, using a receiving antenna with a gain of 0 dBd (2.15 dBi).**

#### 4.3.2.2 Radio Noise

The radio noise experienced by an R-mode receiver has two principal components: (i) *external*, or *environmental*, noise received through the antenna from sources external to the receiving system; (ii) *internal noise* generated by the receiving system itself. Assuming the receiver is installed on a vessel, the environmental noise can further be sub-divided into *man-made noise* generated by sources external to the vessel, and the vessel's *topside noise* generated by on-board machinery and electronic systems. This section aims to quantify the contributions of each of the mentioned categories of noise.

The amount of noise generated by a component in a radio system is commonly specified in terms of the *noise factor*,  $f$ . The noise factor is defined as the ratio of the noise power available at the output terminals of the component to the portion thereof attributable to thermal noise<sup>10</sup> in the input termination at a reference temperature of 290 K. Equivalently, it can be defined as the ratio of the input signal-to-noise ratio to the output signal-to-noise ratio when the input termination is at the reference noise temperature of 290 K. The noise factor expressed in decibels is referred to as the *noise figure*,  $F = 10 \log f$ . The concept of noise factor/figure can also be applied to the receiving antenna, as discussed below.

<sup>10</sup> Noise generated by the thermal agitation of charge carriers inside electrical conductors.

The International Telecommunication Union (ITU) provides statistical data on various types of external radio noise in Recommendation ITU-R P.372 [31]. The recommendation specifies the noise levels in terms of the *external noise figure*, defined as follows:

$$F_a = 10 \log \frac{p_a}{kT_0B},$$

where  $p_a$  is the noise power available from a reference antenna when placed in a given type of environment,  $k$  is the Boltzmann's constant,  $T_0 = 290$  K is the reference temperature, and  $B$  is the measurement bandwidth.

According to Rec. ITU-R P.372, man-made noise levels are expected to vary depending on the type of environment and the frequency band. For a given environment type, the median value of the external noise figure associated with man-made noise,  $F_{am,m}$ , was found to be a linear function of the logarithm of frequency,  $f_c$ :

$$F_{am,m} = c - d \cdot \log f_c.$$

With  $f_c$  expressed in MHz, the constants  $c$  and  $d$  take the values given in Table 12.

Environmental Type	$c$	$d$
City	76.8	27.7
Residential	72.5	27.7
Rural	67.2	27.7

**Table 12: Parameters of the linear model of the median man-made noise [31].**

For  $f_c = 162$  MHz, **the median man-made noise is estimated to be 15.6 dB, 11.3 dB and 6.0 dB above the thermal noise floor ( $kT_0B$ ) for the city, residential and rural environments**, respectively. For coastal navigation, the rural environment value,  $F_{am,m} = 6.0$  dB, seems appropriate from the standpoint of low density of potential sources of man-made noise while at sea and will be used in this analysis.

Note: Man-made noise levels may be expected to be higher near wind farms due to proximity of wind turbine generators and associated electronics and undersea cabling. There is anecdotal evidence suggesting this may be the case; however, no reliable data is currently available to the author to confirm this hypothesis.

The vessel's topside noise is expected to vary depending on the type of vessel and voyage phase. Recommendation ITU-R M.1467 [32] gives representative figures of the topside noise,  $P_{a,v}$ , for three types of vessel, as summarised in Table 13. The Australian Advisory Group for Aeronautical Research and Development (AGARD) figure represents a naval vessel under normal cruise conditions, whilst the Department of Defence (DOD) figure represents the maximum noise level under battle conditions. The figure adopted by the Ionospheric Prediction Service of the Australian Department of Industry (IPS) is generally accepted as representing the noise level encountered on container vessels, pleasure cruisers and utility ships, and is also the value that will be used in this document.

Vessel Type	Topside Noise @ 3 MHz, $P_{a,v}$ (dBW/Hz)	Ext. Noise Figure @ 3 MHz, $F_{a,v}$ (dB)	$c$	$d$
AGARD ship	-148.0	56.0	69.2	27.7
IPS ship	-142.0	62.0	75.2	27.7
DOD Cat. 1 mobile platform	-137.0	67.0	80.2	27.7

**Table 13: Parameters of the linear model of the vessel's topside noise.**

The values of  $P_{a,v}$  given in Table 13 are referenced to an operating frequency of  $f_c = 3$  MHz and a bandwidth of 1 Hz. The table also shows the corresponding external noise figure values,  $F_{a,v}$ , at this operating frequency. Assuming that the topside noise follows the same linear model used for the man-made noise above, with the parameters  $c$  and  $d$  given in Table 13, these figures can be converted to the VHF band. The values of  $c$  in the table were calculated from the value of  $F_{a,v}$  at  $f_c = 3$  MHz assuming that  $d$  (i.e. the slope of the noise figure vs. log-frequency curve) takes the same value as for the man-made noise curves provided in Recommendation ITU-R P.372. For the IPS vessel and  $f_c = 162$  MHz, **the topside noise can then be estimated to be 14.0 dB above the thermal noise floor.**

Combining the topside noise with the median man-made noise value for rural areas gives an external noise figure of  $F_a = 10 \log(10^{F_{a,v}/10} + 10^{F_{am,m}/10}) = 14.6$  dB, which is consistent with recent external noise figure measurements conducted on GLA vessels while moored in the Harwich Harbour, UK (external noise figure values of approximately 10 dB to 27 dB were measured, depending on the vessel and antenna location [33]).

The noise figure values in Recommendation ITU-R P.372 (and presumably in Rec. ITU-R M.1467 too) are referenced to a (hypothetical) short, lossless, vertical monopole antenna above a perfectly conducting ground plane (referred to in the following as the *ITU monopole antenna*). At VHF, a half-wave dipole antenna may be used rather than a monopole; in that case, the external noise figure values may need to be corrected. Rec. ITU-R P.372-12 [34] and report [35] published by the Norwegian Defence Research Establishment suggest that **the external noise figure values should be increased by  $C_a = 3.4$  dB if a half-wave dipole is used** instead of the reference monopole antenna.

The noise levels seen by the receiver are further influenced by the receiving antenna circuit loss,  $L_{c,RX}$ , (representing the conductive and dielectric losses in the antenna) and transmission line loss,  $L_{t,RX}$ . It is assumed here that a tuned antenna is used and therefore the antenna circuit loss is negligible  $L_{c,RX} \approx 0$  dB. The receiver transmission line loss is assumed to have the same value as on the transmitting side,  $L_{t,RX} = L_{t,TX} = 1.2$  dB.

The noise contribution from the receiver itself is given by the receiver's noise figure,  $F_{RX}$ . A value of  $F_{RX} = 10$  dB is assumed based on reference [36].

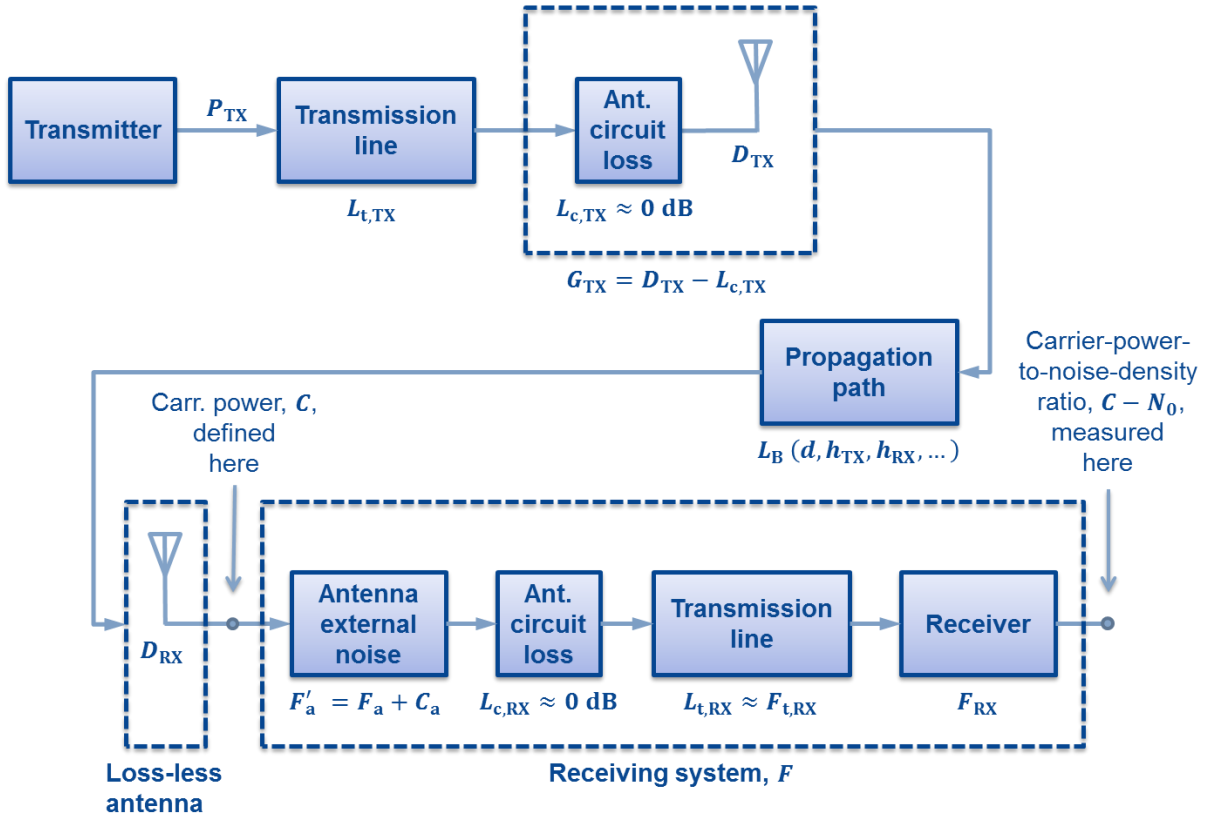


**Figure 6: Noise-equivalent model of the system.**

With reference to Figure 6, the definition of the noise factor and the Friis formula [37], the overall median noise factor of the receiving system, including the effects of the external/environmental and receiver internal noise, can be expressed as follows:

$$f = \underbrace{(f_{am,m} + f_{a,v})}_{f_a} \cdot c_a + (f_{t,RX} - 1) + l_{t,RX} \cdot (f_{RX} - 1),$$

where:

$f_a = 10^{F_a/10}$  is the external noise factor referenced to the ITU monopole antenna;

$f_{am,m} = 10^{F_{am,m}/10}$  is the component of the external noise factor associated with man-made noise;

$f_{a,v} = 10^{F_{a,v}/10}$  is the component of the external noise factor associated with the vessel's topside noise;

$c_a = 10^{C_a/10}$  is the external noise conversion factor for the half-wave dipole antenna;

$f_{t,RX}$  is the noise factor associated with the transmission line loss;

$l_{t,RX} = 10^{L_{t,RX}/10}$  is the loss factor corresponding to the transmission line loss; and

$f_{RX} = 10^{F_{RX}/10}$  is the receiver noise factor.

It can be shown that if the actual temperature of the transmission line is equal to the reference temperature  $T_0 = 290$  K, then  $f_{t,RX} = l_{t,RX}$ , and the above expression can be simplified to:

$$f = (f_{am,m} + f_{a,v}) \cdot c_a - 1 + l_{t,RX} f_{RX}.$$

Substituting for the variables in the above equation (assuming  $F_{am,m} = 6.0$  dB,  $F_{a,v} = 14.0$  dB,  $C_a = 3.4$  dB,  $L_{t,RX} = 1.2$  dB and  $F_{RX} = 10$  dB, as discussed above) yields an overall system noise factor  $f = 75.8$ , corresponding to a system noise figure  $F = 18.8$  dB.

This is consistent with conclusions from the EfficienSea2 VDES sea trials conducted on a passenger ferry operating in the Baltic Sea (the trial system noise figure, including the effects of the external/environmental noise, was estimated to be approximately 17 dB [38]).

Note: Although taking a different approach, the ACCSEAS AIS R-mode study [2] arrived at a similar conclusion with respect to the radio noise levels on ships. The study argued that the AIS requirement of 20% Packet Error Rate (PER) at the minimum signal strength of -107 dBm stated in the AIS technical specification [9] is equivalent (under certain simplifying assumptions) to requiring  $E_S/N_0 = 9.8$  (or 9.9 dB) at the output of the receiver when a signal with the minimum signal strength is applied at its input. In the presence of thermal noise only, the minimum input signal level corresponds to an  $E_S/N_0$  of 27.2 dB at the receiver input, which implies a receiver noise figure of  $F_{RX} = 27.2 - 9.9 = 17.3$  dB. In the ACCSEAS study, this figure was effectively used as an estimate of the system noise figure,  $F$ . It should be noted that a receiving system using a receiver that just meets the AIS requirement will have a system noise figure that is somewhat higher than 17.3 dB due to the transmission line loss and external noise, as discussed above. .

For the purpose of the current study, **the overall system noise figure (incl. the effects of the environmental noise) will be assumed to be  $F = 19$  dB**. This corresponds to a (one-sided) noise power spectral density of

$$N_0 = kT_0 \cdot 10^{\frac{F}{10}} = 3.18 \cdot 10^{-19} \text{ W/Hz},$$

(or -155 dBm/Hz). This value will be used in calculating the received carrier-power-to-noise-density ratio,  $C/N_0$ .

#### 4.3.2.3 Ranging Error vs. Distance

Using the theoretical bounds on the ranging performance derived in Section 4.3.1, the received power vs. distance curves provided in Section 4.3.2.1, and the R-mode receiver noise floor established in Section 4.3.2.2, it is now possible to estimate the VDES ranging error as a function of distance from the VDES R-mode base station.

The figures provided below show the estimated ranging error for the five VDES subsystem configurations, the two R-mode transmission configurations (one-slot vs. maximum-length transmissions) and two representative base station antenna heights (18 m vs. 57 m) considered previously. Additional plots are provided to illustrate the performance gains obtained by combining five successive one-slot transmissions during the range estimation process.

**Caveat: the ranging error predictions shown in this section do not include the effects of multipath propagation, base station synchronisation error and transmission jitter, changing environmental conditions and terrain topography.**

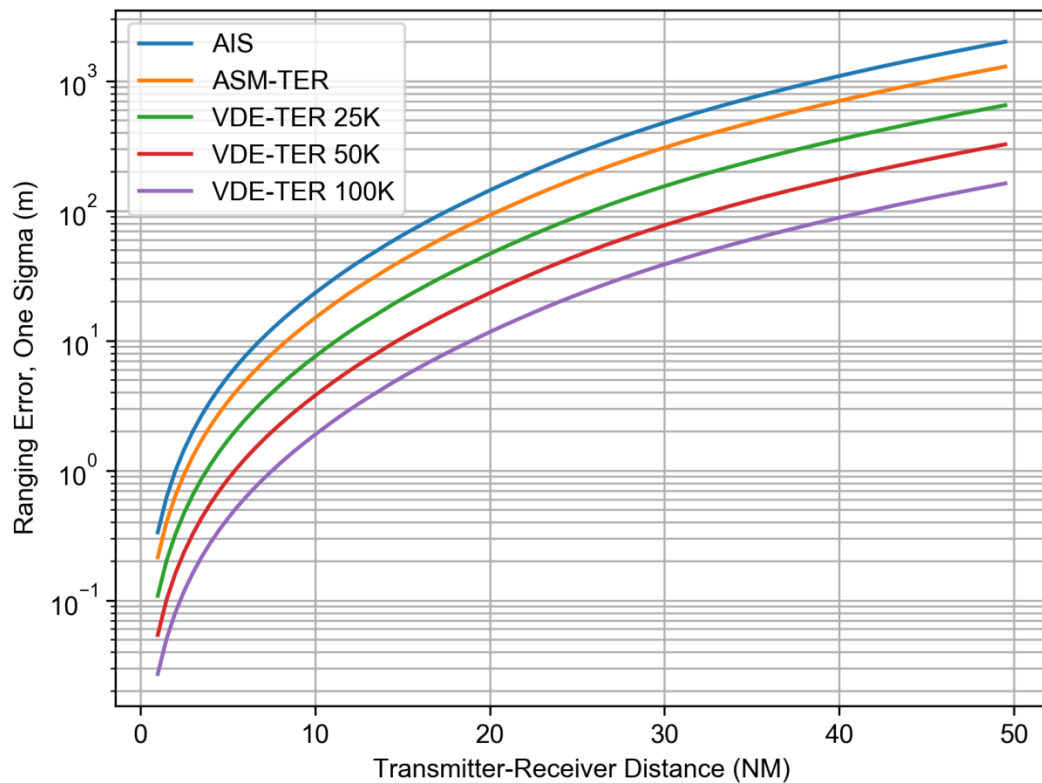


**Figure 7: Ranging error vs. distance; one-slot bursts; base station ant. height: 18 m.**

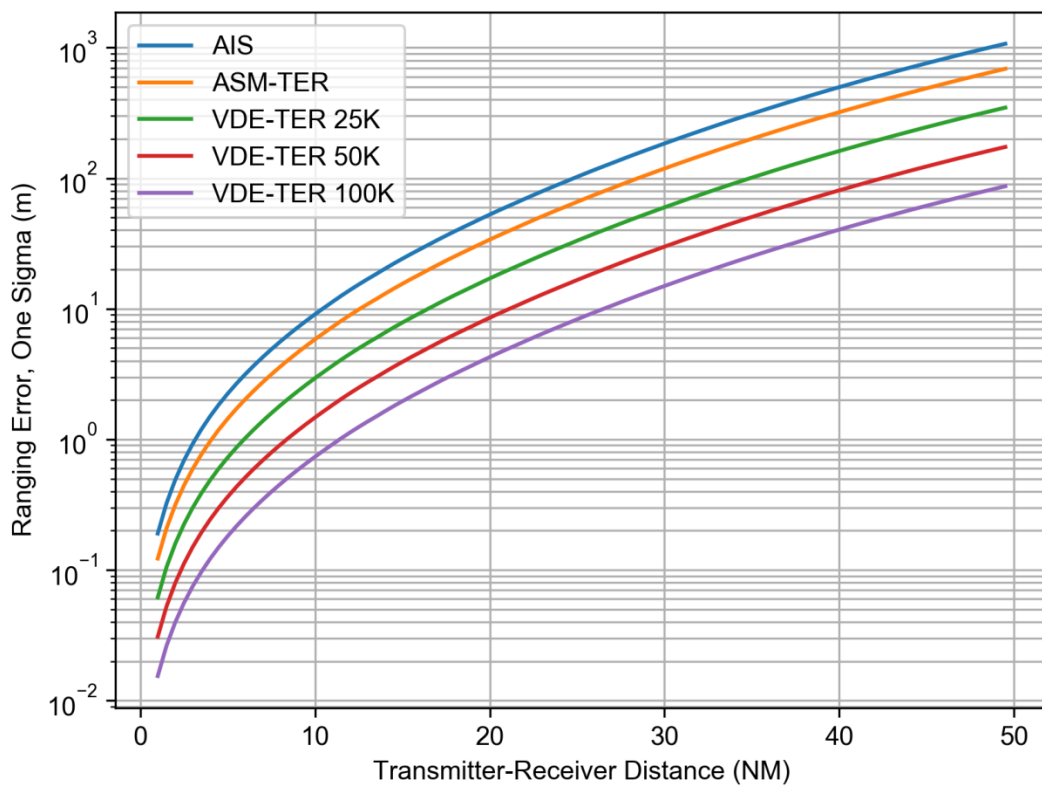


**Figure 8: Ranging error vs. distance; one-slot bursts; base station ant. height: 57 m.**

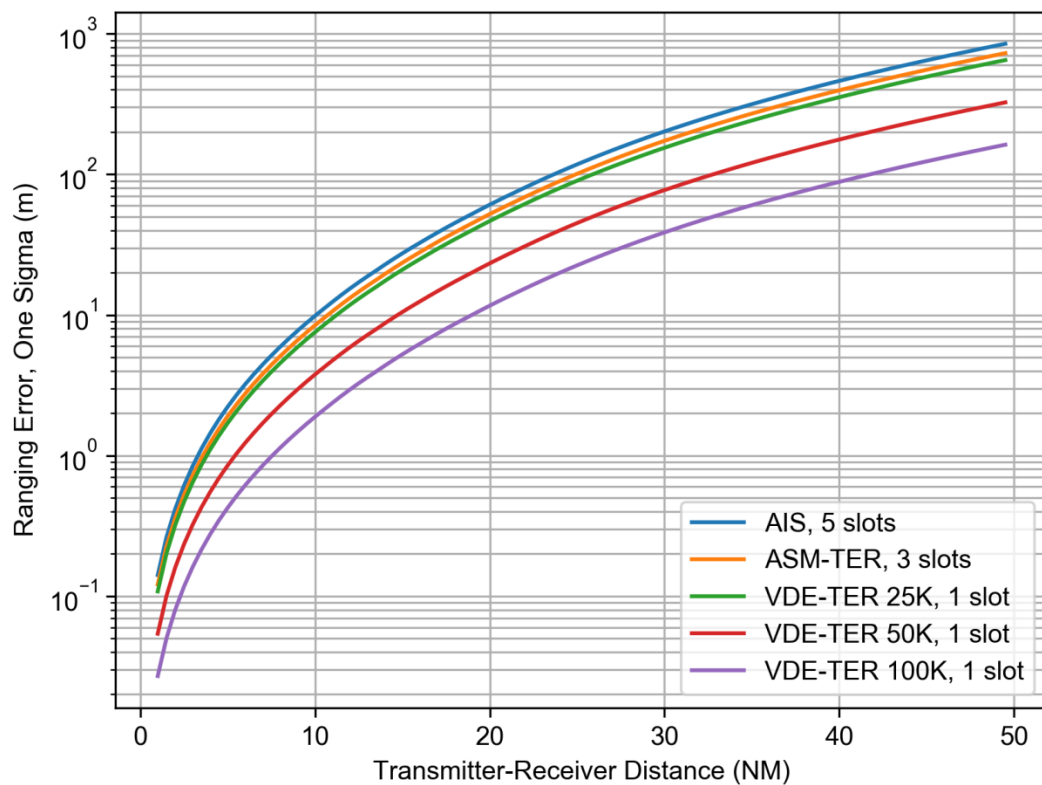


**Figure 9: Ranging error vs. distance; maximum-length bursts; base station antenna height: 18 m.**

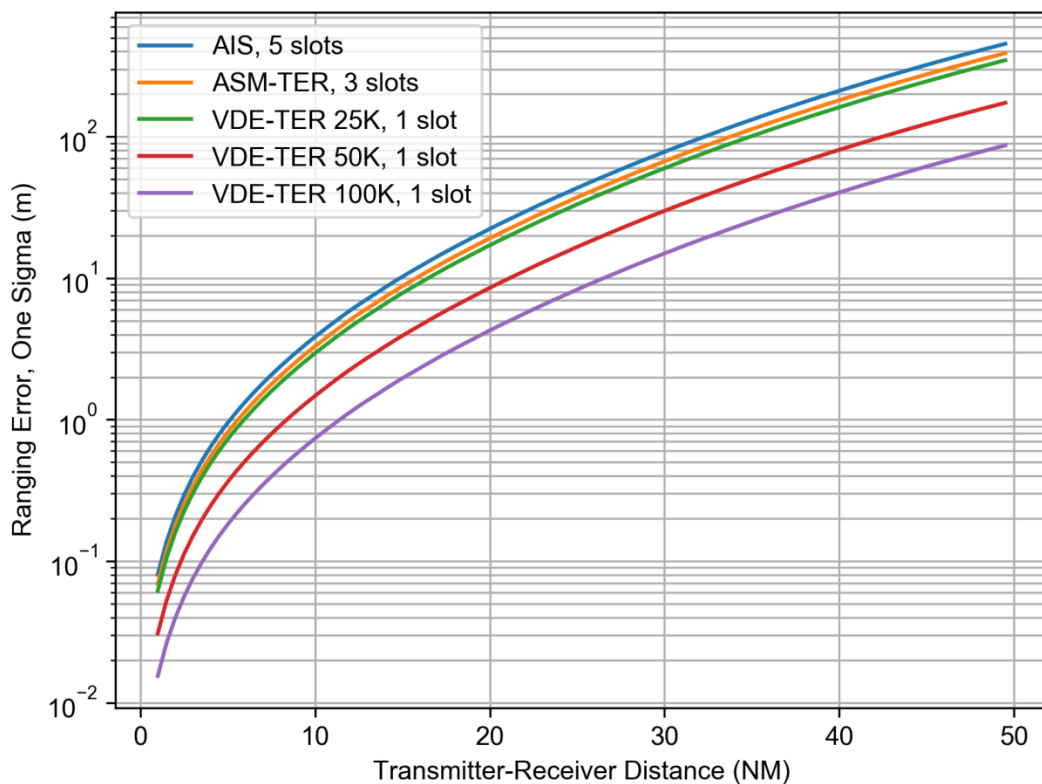


**Figure 10: Ranging error vs. distance; maximum-length bursts; base station antenna height: 57 m.**

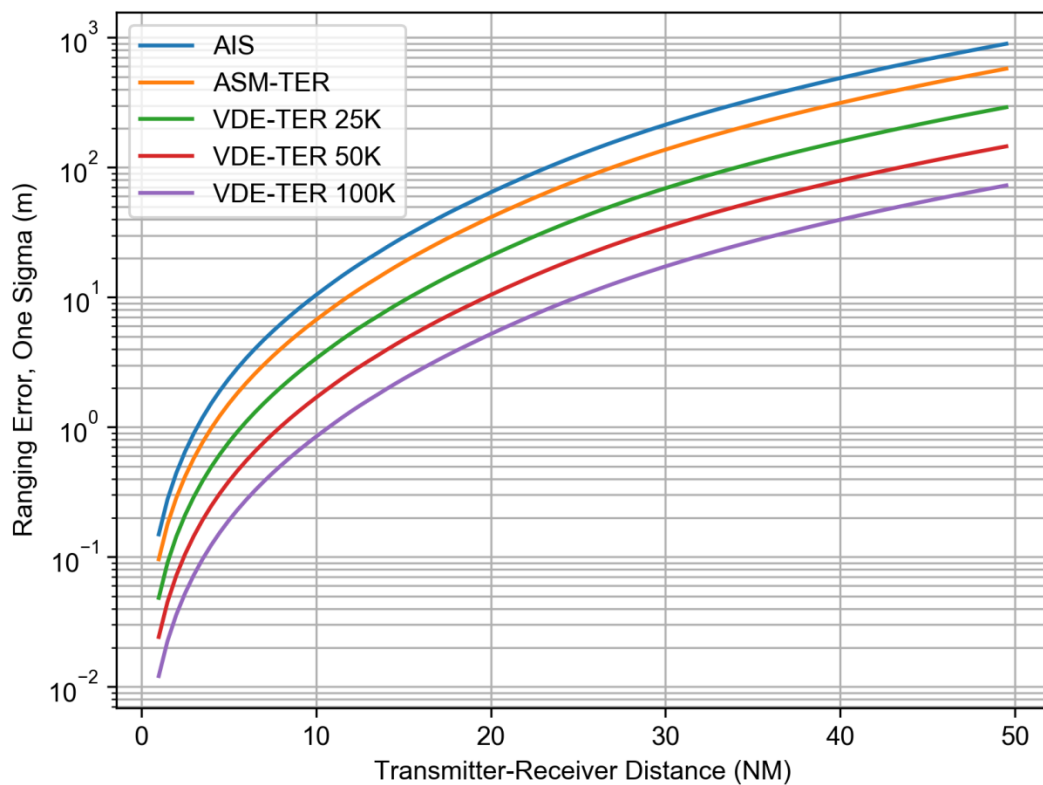


**Figure 11: Ranging error vs. distance; one-slot bursts; receiver integration over 5 slots; base station ant. height: 18 m.**

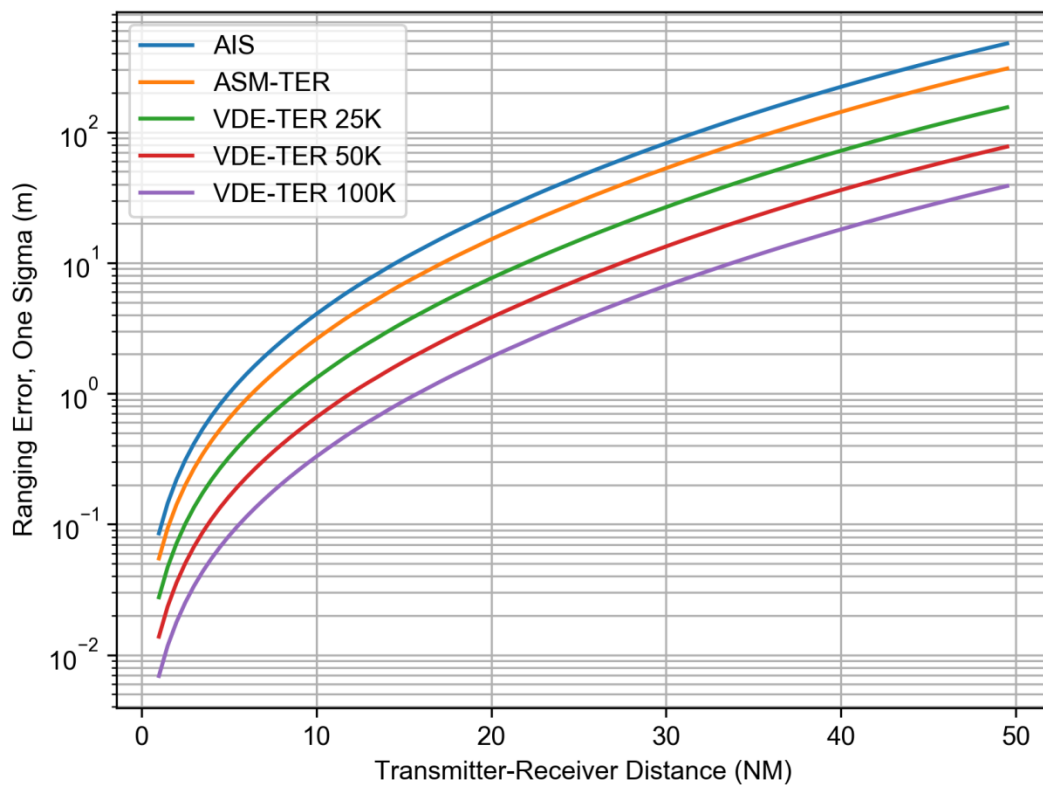


**Figure 12: Ranging error vs. distance; one-slot bursts; receiver integration over 5 slots; base station ant. height: 57 m.**

## 4.4 Discussion

### 4.4.1 Comparison with the ACCSEAS AIS R-mode Model

Several differences between the proposed model for AIS/VDES ranging and the AIS R-mode model presented by the ACCSEAS project have been noted in this document and are summarised below:

- As discussed in Section 4.3.1.1, the expression for the variance of the AIS ranging error derived in the current report is a factor of 2 smaller than the expression derived in the ACCSEAS study.
- The ACCSEAS study assumed that five one-slot transmissions are combined at the receiver, providing  $L_o = 5 \cdot 256 = 1280$  symbols per observation. As can be seen from Table 10, Section 4.3.1.4, the proposed model assumes that a slightly reduced number of symbols are used in the range estimation process,  $L_o = 1120$ , as a certain fraction of symbols within each slot are reserved for transmitter ramp-up/down and a propagation delay guard interval.
- As discussed in Section 4.3.2.2, the ACCSEAS model effectively assumes a system noise figure of 17.3 dB. However, the current analysis assumes a noise figure of 19.0 dB, which seems to be a more realistic assumption, given ITU recommendations related to radio noise and recent noise floor measurements carried out on GLA vessels.

Given the above differences, it is desirable to compare the predicted ranging performance for the two models.

The ACCSEAS model predicts a ranging error of 225 m at the minimum signal strength of -107 dBm and 5.65 m at the signal strength of -75 dBm, as shown in Table 14. The third column in Table 14 shows the error predicted using the newly proposed model, assuming a system noise figure of 17.3 dB; as expected, this is approximately a factor of  $\sqrt{2}$  smaller than the prediction based on the ACCSEAS model due to the difference in the MCRB expressions. The last column in the table shows the predicted error assuming the increased system noise figure of 19.0 dB. As can be seen from the table, these predictions are in relatively good agreement with those of the ACCSEAS project. The differences between the two models thus largely compensate for each other, with the currently proposed model providing slightly more optimistic predictions.

Signal Strength (dBm)	Ranging Error (m, one sigma)		
	ACCSEAS Model, $L_o = 1280$	Proposed Model, assuming System NF of 17.3 dB and $L_o = 1120$	Proposed Model, assuming System NF of 19 dB and $L_o = 1120$
-107	225	170	206
-75	5.65	4.26	5.18

**Table 14: Comparison of the proposed model for AIS ranging error with the ACCSEAS model.**

Experiment	Number of Symbols per Observation	Transmitter-receiver Separation (NM)	Ranging Error from Experimental Results (m, one sigma)	Ranging Error Calculated with the Proposed AIS Ranging Error Model <sup>11</sup> (m, one sigma)
Xinghai Bay [3]	224 <sup>12</sup>	$\approx 2.0$ <sup>13</sup>	3.0 <sup>14</sup>	1.1
Xinghai Bay – Mooring [4]	224	$\approx 2.0$	4.1	1.1
Xinghai Bay – Laopian Island [4]	224	$\approx 4.6$	4.2	5.1
Xinghai Bay – one-slot bursts [5]	224	$\approx 4.3$	60	4.5
Xinghai Bay – five-slot bursts [5]	1064	$\approx 4.3$	28	2.1

**Table 15: Comparison of the proposed AIS ranging error model with experimental results published by the DMU.**

#### 4.4.2 Comparison with Measurement Results

Table 15 above compares predictions obtained using the model for the AIS ranging error proposed in this document with experimental results published by the DMU. As can be seen from the table, the model generally underestimates the measurement error. This is expected, as the model does not yet include the effects of transmitter synchronisation error and multipath propagation, which are expected to dominate the error budget at short ranges, as well as other potential sources of error.

The reason for the significantly larger measurement errors reported in reference [5] (rows 5 and 6 in Table 15) is not clear but may be because ‘ASF corrections’ may not have been applied in these particular experiments.

#### 4.4.3 Maximum Usable Range and Achievable Coverage

Assuming that AIS/VDES R-mode is realised as a standalone passive ranging system with a position accuracy target,  $a_{\text{DRMS}}$ , in the low tens of meters, and that favourable base station geometry can be guaranteed ( $HDOP < 2$ ), then the ranging error for each station included in the position solution must be no greater than approximately  $a_{\text{DRMS}}/HDOP \approx 20/2 = 10$  m.

Table 16 shows the estimated maximum transmitter-receiver separation at which a 10 m ranging error can be achieved, for the AIS (worst performance) and the VDE-TER 100K (best performance) R-mode system configurations, two representative base station antenna heights, and assuming that the R-mode receiver integrates over five one-slot transmissions. As can be seen from the table, **the maximum usable range for AIS-based R-mode is**

<sup>11</sup> Assuming transmitting antenna height of 18 m a. s. l. and receiving antenna height of 10 m.

<sup>12</sup> Assuming measurements were based on one-slot transmissions.

<sup>13</sup> Estimated from the transmitter geometry and HDOP stated in the reference.

<sup>14</sup> Estimated from the stated HDOP and position error.

**expected to be between 10 NM and 15 NM. If one of the new VDE-TER 100K waveforms is used instead of AIS, the maximum range is expected to increase to about 25 NM to 34 NM.** These figures, along with the known distribution of existing (and planned) AIS base stations in the UK and Ireland, can now be used to provide an initial estimate of the achievable AIS/VDES R-mode coverage in the waters around the British Isles.

Figure 13 shows the simultaneous availability of three (left) and two (right) base stations (supporting positioning by passive and active ranging, resp.) assuming maximum station range of 14 NM (26 km), corresponding to the estimated maximum range for AIS-based R-mode. As is apparent from the figure, **there is an insufficient number of base stations to provide 10-m-level AIS R-mode service coverage along the UK and Irish coasts.**

Figure 14, showing the simultaneous base station availability for the VDE-TER 100K configuration, provides a more encouraging picture. The figure suggests that **there may be sufficient station availability along the north and west coast of Scotland, south-east of England and along a significant portion of the Irish coastline (assuming all existing and planned AIS base stations are converted to VDES).** However, even with the new VDES waveforms, additional base stations would need to be deployed in certain parts of the GLA' service area in order to achieve contiguous coverage.

The figures also clearly show the potential improvement in coverage that could be achieved by using alternative positioning techniques that require only two stations to form a position solution (such as positioning by active ranging).

Note: the station database used to generate the station availability plots includes all existing AIS base stations in the UK and Ireland operated by the MCA and CIL/IRCG, as well as the planned stations of the TH Virtual AIS AtoN network; a total of 119 stations.

	Range @ 10 m Error for BS Ant. Height of 18 m a. s. l. (NM)		Range @ 10 m Error for BS Ant. Height of 57 m a. s. l. (NM)	
Transmission Configuration	AIS	VDE-TER 100K	AIS	VDE-TER 100K
One-slot Bursts	6.9	19.0	10.4	26.5
Max-length Bursts	10.1	19.0	14.9	26.5
Integrating 5 One-slot Bursts	9.8	24.9	14.6	33.8

**Table 16: Estimated maximum transmitter-receiver separation for 10 m ranging error.**

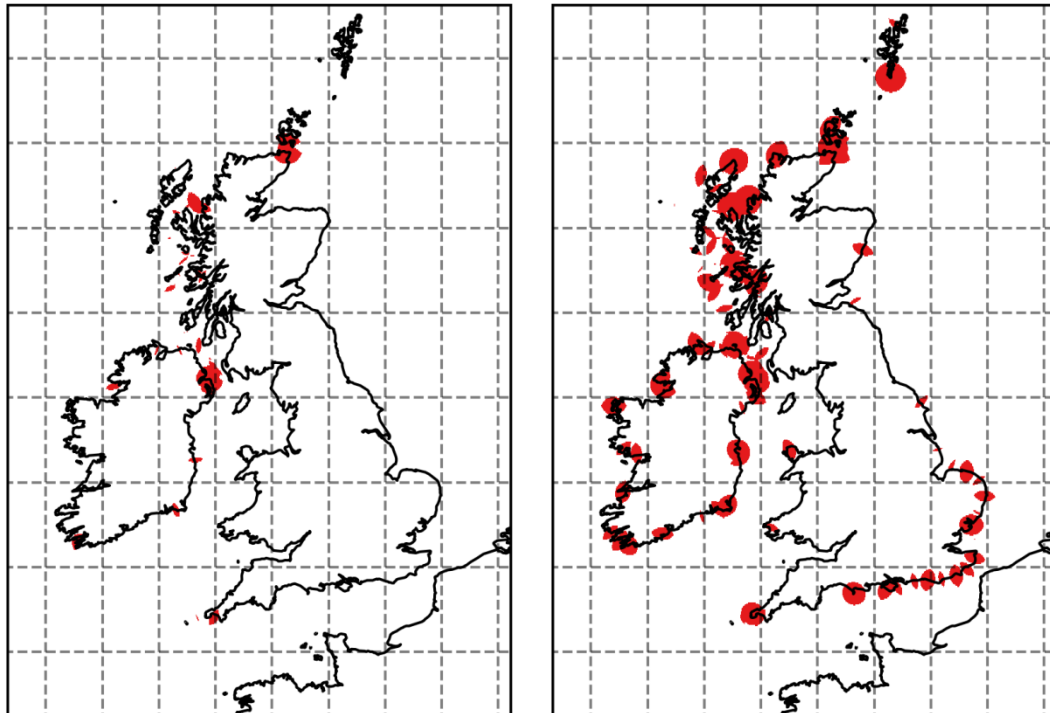


**Figure 13: Simultaneous availability of 3 (left) and 2 (right) R-mode base stations (supporting positioning by passive and active ranging, resp.), assuming maximum usable station range of 15 NM (AIS waveform).**

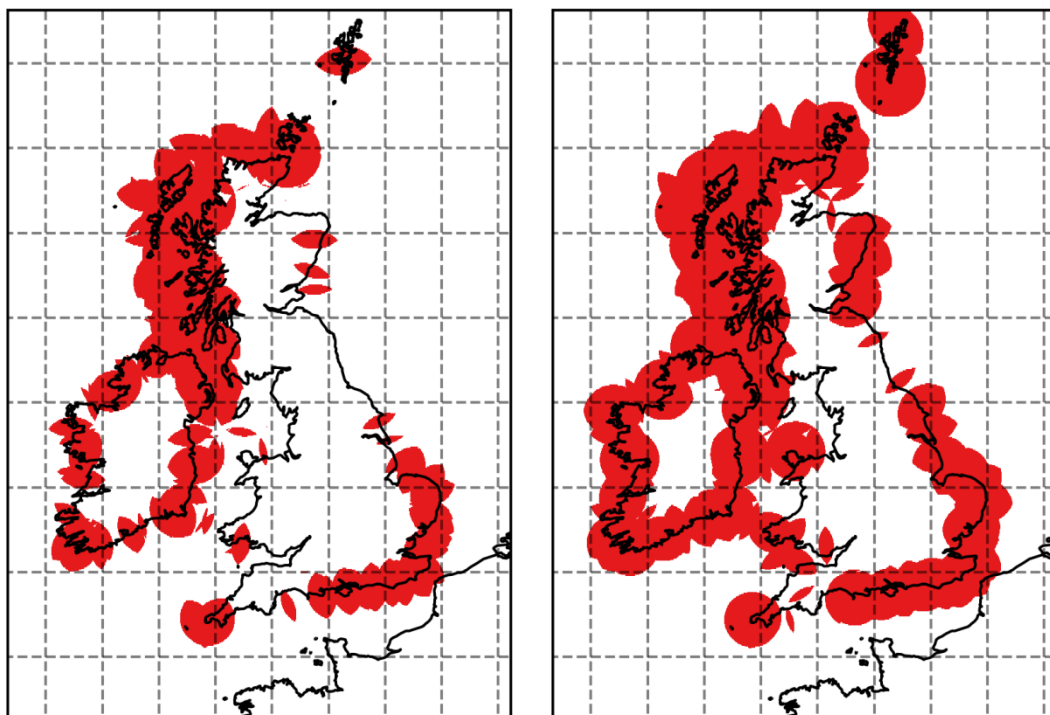


**Figure 14: Simultaneous availability of 3 (left) and 2 (right) R-mode base stations (supporting positioning by passive and active ranging, resp.), assuming maximum usable station range of 34 NM (VDE-TER 100K waveforms).**

## 5 Recommendations for Future Work

Following the literature review in Section 2 and identification of gaps in Section 3, a number of recommendations with respect to future R-mode development were given in Section 3.7. The first two recommendations ('Focus on VDES R-mode rather than AIS R-mode' and 'Determine the achievable ranging performance under realistic propagation conditions and transmitter-receiver separations') were subsequently addressed in Section 4.

Given the results of the initial theoretical analysis in Section 4, it is recommended that further work in this area should:

- Consider the use of tighter performance bounds, such as the Ziv-Zakai bound, instead of the MCRB; the MCRB is known to provide overly optimistic estimates in the low-to-medium SNR region;
- Include the effects of multipath propagation in the ranging performance model;
- Include the effects of transmitter synchronisation error in the performance model;
- Study the effects of changing environmental conditions on the signal propagation speed;
- Study the effects of topography on the signal propagation delay;
- If the decision is made to use dedicated R-mode transmissions (as opposed to ranging off ordinary user data transmissions), investigate potential performance gains to be obtained by optimising the transmission data sequence.

The initial analysis suggests that achieving a contiguous R-mode coverage along the UK and Irish coasts using a passive ranging architecture would require a significant expansion of the existing AIS transmission network. In order to minimise the need for new stations, it is recommended that future work considers alternative positioning methods, such as active ranging, or passive ranging aided with high-stability receiver clock, which require only two stations to form a position solution.

For the remaining steps of the proposed VDES R-mode development roadmap see Section 3.7.

It is recommended that the results of this preliminary work are disseminated to the relevant decision makers.

## References

- [1] G. Johnson and P. Swaszek, 'Feasibility Study of R-Mode Using AIS Transmissions', May 2014.
- [2] G. Johnson and P. Swaszek, 'Feasibility Study of R-Mode Using AIS Transmissions', Aug. 2014.
- [3] Q. Hu, Y. Jiang, J. Zhang, X. Sun, and S. Zhang, 'Development of an Automatic Identification System Autonomous Positioning System', *Sensors (Basel, Switzerland)*, vol. 15, pp. 28574–28591, Nov. 2015.
- [4] K. Zheng, Q. Hu, and J. Zhang, 'Positioning Error Analysis of Ranging-Mode Using AIS Signals in China', *Journal of Sensors, Hindawi*, vol. 2016, Aug. 2016.
- [5] J. Zhang, S. Zhang, and J. Wang, 'Pseudorange Measurement Method Based on AIS Signals', *Sensors (Basel, Switzerland)*, vol. 17, May 2017.
- [6] X. Wang, S. Zhang, and X. Sun, 'The Additional Secondary Phase Correction System for AIS Signals', *Sensors (Basel, Switzerland)*, vol. 17, Mar. 2017.
- [7] 'True Heading AB (publ) has been granted a patent', *TrueHeading.se*, Sep-2015. [Online]. Available: [http://www.trueheading.se/files/document/thecompany/newsandpr/pressmeddelande\\_true-heading\\_150910\\_new-patent\\_e.pdf](http://www.trueheading.se/files/document/thecompany/newsandpr/pressmeddelande_true-heading_150910_new-patent_e.pdf).
- [8] P. D. Groves, 'Review of Combined Technology Options for Maritime Resilient PNT', Report to the Research & Radionavigation Directorate of the General Lighthouse Authorities of the United Kingdom and Ireland, Mar. 2017.
- [9] ITU, 'Technical Characteristics for an Automatic Identification System Using Time Division Multiple Access in the VHF Maritime Mobile Frequency Band', Recommendation ITU-R M.1371-5, Feb. 2014.
- [10] S. Kondapalli, 'China's Naval Strategy', *The Institute for Defence Studies and Analyses*, Apr-2018. [Online]. Available: <https://www.idsa-india.org/an-mar00-3.html>.
- [11] IALA, 'The Technical Specification of VDES', IALA Guideline No. 1139, Edition 1.0, Dec. 2017.
- [12] ITU, 'Method for Point-to-Area Predictions for Terrestrial Services in the Frequency Range 30 MHz to 3 000 MHz', Rec. ITU-R P.1546-5, Sep. 2013.
- [13] ITU, 'A Path-Specific Propagation Prediction Method for Point-to-Area Terrestrial Services in the VHF and UHF Bands', ITU-R P.1812-4, Jul. 2015.
- [14] J. Safar, D. Haley, A. Pollok, R. Luppino, A. Grant, and N. Ward, 'VDES Channel Sounding Campaign', General Lighthouse Authorities of the UK and Ireland, 2014.
- [15] ITU, 'VHF Data Exchange System Channel Sounding Campaign', Geneva, Switzerland, Report ITU-R M.2317-0, Nov. 2014.
- [16] JRC, 'Investigation of Multipath Fading for VDES', presented at the 2nd JCG Workshop on VDES, Tokyo, Japan, Jan-2014.
- [17] JRC, 'Test Report of Radio Path in Tokyo Bay', Feb. 2016.
- [18] 'Measurement System for Additional Secondary Phase Factor of VHF Signal', Patent CN 103439687 A.
- [19] D. E. Kerr, *Propagation of Short Radio Waves*. McGraw-Hill, 1951.
- [20] J. M. Richards, 'A Simple Expression for the Saturation Vapour Pressure of Water in the Range  $-50$  to  $140^{\circ}\text{C}$ ', *Journal of Physics D: Applied Physics*, vol. 4, no. 4, 1971.

- [21] M. Morelli and U. Mengali, 'Joint Frequency and Timing Recovery for MSK-Type Modulation', *IEEE Transactions on Communications*, vol. 47, p. 9, Jun. 1999.
- [22] M. Morelli and G. M. Vitetta, 'Joint Phase and Timing Recovery for MSK-Type Signals', *IEEE Transactions on Communications*, vol. 48, Dec. 2000.
- [23] S. Sezginer, 'Symbol Synchronization for MSK Signals based on Matched Filtering', MSEE, Graduate School of Natural and Applied Sciences, Middle East Technical University, 2003.
- [24] U. Mengali and A. N. D'Andrea, *Synchronization Techniques for Digital Receivers*. Plenum Press, New York, 1997.
- [25] IMO, 'Resolution A.1046(27), World Wide Radionavigation System', Dec. 2011.
- [26] IMO, 'Resolution A.915(22) on Revised Maritime Policy and Requirements for a Future Global Navigation Satellite System (GNSS)', Nov. 2001.
- [27] P. D. Groves, *Principles of GNSS, Inertial, and Multisensor Integrated Navigation Systems*. Artech House, 2008.
- [28] ITU, 'Automatic Identification System VHF Data Link Loading', Report ITU-R M.2287-0, Dec. 2013.
- [29] J. Sykora, *Teorie digitalni komunikace*. Czech Technical University, Prague, 2003.
- [30] 'Poisson Summation Formula', *Wikipedia*, Apr-2018. [Online]. Available: [https://en.wikipedia.org/wiki/Poisson\\_summation\\_formula](https://en.wikipedia.org/wiki/Poisson_summation_formula).
- [31] ITU, 'Radio Noise', International Telecommunication Union, Rec. ITU-R P.372-13, Sep. 2016.
- [32] *ITU-R M.1467-1, Prediction of Sea Area A2 and NAVTEX Ranges and Protection of the A2 Global Maritime Distress and Safety System Distress Watch Channel*. International Telecommunication Union, 2006.
- [33] J. Safar, 'VDES Development and Applications (FY17-18)', General Lighthouse Authorities of the UK and Ireland, R&RNAV Directorate, Technical Report, To be published.
- [34] ITU, 'Radio Noise', International Telecommunication Union, Rec. ITU-R P.372-12, Jul. 2015.
- [35] B. Skeie and B. Solberg, 'External Man-made Radio Noise Measurements', Norwegian Defence Research Establishment, 16/00869, Oct. 2016.
- [36] True Heading, 'AIS RX PRO Datasheet', Apr-2018. [Online]. Available: [http://www.trueheading.se/files/document/products/ais/aisrxpro/AIS%20RX%20PRO\\_20130913.pdf](http://www.trueheading.se/files/document/products/ais/aisrxpro/AIS%20RX%20PRO_20130913.pdf).
- [37] 'Friis Formula for Noise', *Wikipedia*, Apr-2018. [Online]. Available: [https://en.wikipedia.org/wiki/Friis\\_formulas\\_for\\_noise](https://en.wikipedia.org/wiki/Friis_formulas_for_noise).
- [38] K. Bronk, 'E-mail correspondence between J. Safar and K. Bronk', Mar-2018.